

**Exceptional Event Demonstration for
Ozone Exceedances in Clark County,
Nevada: June 27, 2018**

September 2021

Clark County Department of Environment and Sustainability
4701 West Russell Road, Suite 200
Las Vegas, NV 89118
(702) 455-5942

TABLE OF CONTENTS

1.0 OVERVIEW 1-1

1.1 Introduction..... 1-1

1.2 Exceptional Event Demonstration Criteria 1-2

1.3 Regulatory Significance of the Exclusion..... 1-4

2.0 AREA DESCRIPTION AND CHARACTERISTICS OF NON-EVENT OZONE FORMATION 2-1

2.1 Area Description 2-1

2.2 Characteristics of Non-Event Ozone Formation..... 2-4

2.2.1 Emission Trend 2-4

2.2.2 Weather Patterns Leading to Ozone Formation..... 2-7

2.2.3 Weekday and Weekend Effect..... 2-7

3.0 EVENT SUMMARY AND CONCEPTUAL MODEL..... 3-1

3.1 Previous Research on Ozone Formation and Smoke Impacts 3-1

3.2 California Wildfires in 2018 3-1

3.3 June 27, 2018 3-2

4.0 CLEAR CAUSAL RELATIONSHIP 4-1

4.1 Analysis Approach..... 4-1

4.2 Comparison of Event-Related Concentrations with Historical Concentrations .. 4-2

4.3 Event of June 27, 2018..... 4-8

4.3.1 Tier 1 Analysis: Historical Concentrations..... 4-8

4.3.2 Tier 2 Analysis..... 4-9

4.3.2.1 Key Factor #2..... 4-9

4.3.2.2 Evidence of Fire Emissions Transport to Area Monitors 4-9

4.3.2.3 Evidence that Fire Emissions Affected Area Monitors 4-14

4.3.3 Tier 3 Analysis: Additional Weight of Evidence to Support Clear Causal Relationship 4-19

4.3.3.1 GAM Statistical Modeling..... 4-19

5.0 NATURAL EVENT 5-1

6.0 NOT REASONABLY CONTROLLABLE OR PREVENTABLE 6-1

7.0 CONCLUSIONS 7-1

8.0 REFERENCES..... 8-1

APPENDIX A: EXCEPTIONAL EVENT INITIAL NOTIFICATION FORM

APPENDIX B: PUBLIC NOTIFICATION

APPENDIX C: DOCUMENTATION OF PUBLIC COMMENT PROCESS

LIST OF FIGURES

Figure 1-1. Relationship between Total Burned Area in California and Number of Exceedance Days in Clark County in Summer Months (May–August), 2014–2018. 1-1

Figure 1-2. Relationship between Log Value of Total Burned Area and Number of Exceedance Days in Summer Months of 2018. 1-1

Figure 2-1. Mountain Ranges and Hydrographic Areas Surrounding the Las Vegas Valley. 2-1

Figure 2-2. Clark County O₃ Monitoring Network. 2-2

Figure 2-3. Locations of FEM PM_{2.5} Monitors. 2-3

Figure 2-4. Locations of FRM PM_{2.5} Monitors. 2-4

Figure 2-5. Typical Summer Weekday NO_x. 2-5

Figure 2-6. Typical Summer Weekday VOCs. 2-5

Figure 2-7. Anthropogenic Emission Trends of NO_x and VOC in California, 2008–2019. ... 2-5

Figure 2-8. Anthropogenic Emission Trends of NO_x and VOCs in Clark County, 2008–2017. 2-6

Figure 2-9. Eight-hour Ozone 4th Highest Average at Monitors in Clark County, 2009–2019. 2-6

Figure 2-10. Typical Ozone Season 1-Hour Ozone Diurnal Pattern for 50th and 95th Percentile Values at Clark County Monitors. 2-7

Figure 2-11. Locations of NO₂ Monitors. 2-8

Figure 2-12. Weekly Pattern for 1-Hour NO₂ at Monitors from 2014–2019 (May-August). ... 2-8

Figure 2-13. Weekly Pattern for 24-Hour NO₂ average at Monitors from 2014–2019 (May-August). 2-9

Figure 2-14. Weekly Pattern for MDA8 O₃ Average at Monitors, 2014–2019 (May–August). 2-9

Figure 3-1. Difference (“Fire” / “No Fire”) in Maximum 8-hour Ozone for June 25, 2005. 3-1

Figure 3-2. Number of Fires and Acres Burned by Month. 3-2

Figure 3-3. MDA8 Ozone Levels at LVV Monitors during 2018 Ozone Season. 3-2

Figure 3-4. NOAA Daily Hazard Mapping System Smoke Analysis on June 24 (top) and June 25 (bottom). 3-3

Figure 3-5. 500-mb Weather Patterns at 7 AM EST, June 24–27. 3-4

Figure 3-6. Surface Maps at 7 AM EST, June 25-27. 3-5

Figure 3-7. 850-mb Weather Patterns at 12 UTC for June 25-27. 3-6

Figure 3-8. Upper LVV Weather: Skew-T diagrams at 12Z on June 26–27. 3-7

Figure 3-9. Surface LVV Weather, June 25–27. 3-8

Figure 3-10. Simple Conceptual Model of June 27 Wildfire-Influenced Ozone Event. 3-8

Figure 4-1. Cumulative Frequency of Daily Maximum Temperature, Daily Average Wind Speed, and Daily Average Relative Humidity at McCarran International Airport, 2014–2018. 4-3

Figure 4-2. Distribution of Days by MDA8 Ozone Levels, 2014–2018. 4-3

Figure 4-3. MDA8 Ozone at Paul Meyer, 2018 Ozone Season. 4-4

Figure 4-4. MDA8 Ozone at Walter Johnson, 2018 Ozone Season. 4-4

Figure 4-5. MDA8 Ozone at Joe Neal, 2018 Ozone Season. 4-5

Figure 4-6. MDA8 Ozone at Green Valley, 2018 Ozone Season. 4-5

Figure 4-7. MDA8 Ozone at Palo Verde, 2018 Ozone Season. 4-6

Figure 4-8. MDA8 Ozone at Jerome Mack, 2018 Ozone Season. 4-6

Figure 4-9. OC/EC Ratio at Jerome Mack, 2018–2019 Ozone Season..... 4-7
Figure 4-10. OC/EC ratio at Rubidoux, CA, 2018–2019 Ozone Season. 4-7
Figure 4-11. 5-Year Hourly Seasonal 95th & 50th Percentiles for O₃ and Observed O₃ on June 27. 4-8
Figure 4-12. Visible Satellite Imagery, June 24–26. 4-10
Figure 4-13. MODIS (Aqua/Terra) AOD Retrievals for June 25..... 4-11
Figure 4-14. MODIS (Aqua/Terra) AOD Retrievals for June 26..... 4-12
Figure 4-15. MODIS (Aqua/Terra) AOD Retrievals for June 27..... 4-12
Figure 4-16. 48-hr Backward Trajectories at GV, JM, and WJ, 2 AM and 1 PM PST, June 25. 4-13
Figure 4-17. 48-hr Backward Trajectories at GV, JM, and WJ, 2 AM and 1 PM PST, June 26. 4-14
Figure 4-18. 48-hr Backward Trajectories at GV, JM, and WJ, 2 AM and 1 PM PST, June 27. 4-14
Figure 4-19. Monitors Outside the Las Vegas Valley. 4-15
Figure 4-20. MDA8 O₃ at Monitors Outside the LVV, June 25–28..... 4-15
Figure 4-21. MDA8 O₃ at Monitors Inside the LVV, June 25–28. 4-16
Figure 4-22. Time Series of 1-Hour Ozone Readings for Death Valley, June 25–28..... 4-16
Figure 4-23. Time Series of 1-Hour Ozone Readings for Great Basin, June 25–28. 4-16
Figure 4-24. Actual and Mean OC/EC ratio at Jerome Mack and Rubidoux, CA, and Daily 24-hour PM_{2.5} at Jerome Mack, June 25–28, 2018. 4-17
Figure 4-25. Hourly O₃ Concentrations at Jerome Mack, June 25–28. 4-18
Figure 4-26. Hourly NO₂ Concentrations at Jerome Mack, June 25–28. 4-18
Figure 4-27. Hourly PM_{2.5} Concentrations at Jerome Mack, June 25–28. 4-18
Figure 4-28. Observed and Predicted MDA8 O₃ at Exceeding Monitors, June 24–28. 4-20

LIST OF TABLES

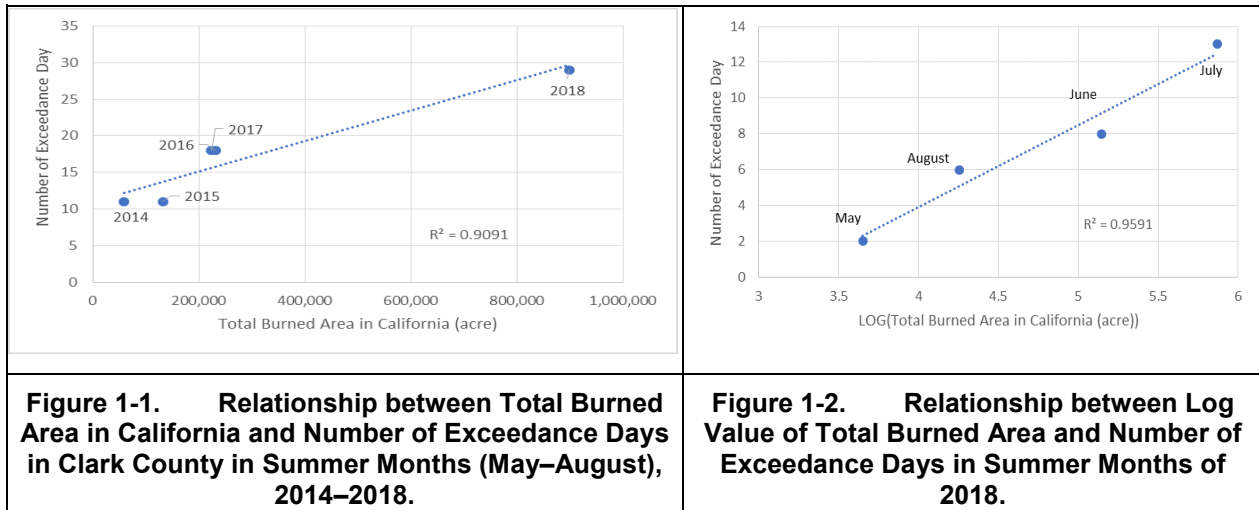
Table 1-1. Ozone Monitors Proposed for Data Exclusion 1-2
Table 1-2. Impact of Wildfire Events on Design Values of 2018–2020 (all values in ppb)..... 1-4
Table 4-1. June 19–20 GAM Results for Exceeding Sites..... 4-20
Table 5-1. Basic Information for Wildfire Events on June 19-20, 2018..... 5-1

1.0 OVERVIEW

1.1 INTRODUCTION

Ozone (O₃) exceedances in Clark County are frequently influenced by surrounding wildfires. In the proper weather conditions, wildfire emissions can travel hundreds of miles from the point of origin. This is especially true of wildfires in California, which cause more exceedances of the National Ambient Air Quality Standard (NAAQS) for ozone in Clark County than fires in other areas because of regionally predominant winds that flow from California to the Las Vegas Valley (LVV) in summer.

Figure 1-1 uses data from annual “Wildland Fire Summary” reports (2014–2018) from the National Interagency Coordination Center (NICC) to show the strong relationship between the number of ozone exceedance days in Clark County and the total area in California burned by wildfires ($R^2 = 0.9091$). The 2018 fire season in California was the most destructive on record, with the NICC reporting a total of 8,054 fires burning an area of 1,823,153 acres. Figure 1-2 shows the high correlation between the area burned (logarithmic value) in California and the number of ozone exceedance days in Clark County from May to August 2018 ($R^2 = 0.9591$), based on the “2018 Wildfire Activity Statistics” report published by the California Department of Forestry and Fire Protection (CAL FIRE). Though it represents only the areas of the state for which CAL FIRE was responsible, that was more than 50% of the total burned area in California.



With that background in mind, the Clark County Department of Environment and Sustainability (DES) is concurrently submitting several exceptional events demonstrations of ozone concentrations that exceeded the 2015 ozone NAAQS due to smoke impact on the days in 2018 listed in Table 1-1. All have been prepared consistent with Title 40, Part 50 of the Code of Federal Regulations (40 CFR 50).

This document is submitted for the June 27, 2018, event influenced by smoke from the Pawnee Fire, Lane Fire, and Lions Fire in California and Mexico/California border wildfires.

The submittal process began with an Exceptional Events Initial Notification sent to EPA Region 9 on November 30, 2020 (Appendix A). With this demonstration package, DES petitions the Regional Administrator for Region 9 of the U.S. Environmental Protection Agency (EPA) to exclude air quality monitoring data for ozone on June 27, 2018, from the normal planning and regulatory requirements under the Clean Air Act (CAA) in accordance with the Exceptional Events Rule (EER), codified at 40 CFR 50.1, 50.14, and 51.930.

Table 1-1 lists the maximum daily 8-hour average of ozone (MDA8 ozone) at network monitors on the exceedance days.

Table 1-1. Ozone Monitors Proposed for Data Exclusion

| AQSID ¹ | 320030043 | 320030071 | 320030073 | 320030075 | 320030298 | 320030540 |
|-----------------------|------------|----------------|------------|-----------|--------------|-------------|
| Date | Paul Meyer | Walter Johnson | Palo Verde | Joe Neal | Green Valley | Jerome Mack |
| 20180619 ² | 72 (10) | 72 (14) | — | — | 77 (4) | 75 (4) |
| 20180620 | 71 (15) | 74 (9) | — | 72 (10) | — | — |
| 20180623 | 72 (7) | 76 (4) | 71 (5) | 72 (9) | 75 (6) | 72 (10) |
| 20180627 | 75 (4) | 76 (4) | 72 (3) | 72 (8) | 78 (1) | 76 (3) |
| 20180714 | 72 (13) | — | — | — | 78 (3) | 78 (1) |
| 20180715 | — | 71 (21) | — | 78 (2) | 73 (11) | 73 (7) |
| 20180716 | 75 (3) | 79 (1) | 75 (1) | 80 (1) | 71 (19) | 73 (8) |
| 20180717 | 74 (5) | 77 (3) | 74 (2) | — | — | — |
| 20180725 | 71 (17) | 72 (15) | — | — | 72 (14) | — |
| 20180726 | 72 (8) | 75 (6) | 70 (6) | — | 77 (4) | 77 (2) |
| 20180727 | 72 (9) | 74 (11) | 70 (7) | 76 (4) | — | — |
| 20180730 | — | — | — | — | 73 (11) | 72 (11) |
| 20180731 | — | 73 (13) | — | 73 (6) | — | — |
| 20180806 | 79 (1) | 77 (2) | 72 (4) | 76 (3) | 74 (10) | 71 (12) |
| 20180807 | 73 (6) | 74 (7) | — | 74 (5) | 72 (16) | 71 (13) |

¹Air Quality System identification numbers (AQSID) and local names identify key monitors.

²MDA8 ozone is listed in parts per billion (ppb) with Tier 2, Key Factor 2 ranking of measurement for 2018 season in parentheses.

1.2 EXCEPTIONAL EVENT DEMONSTRATION CRITERIA

40 CFR 50.1(j) states:

Exceptional event means an event(s) and its resulting emissions that affect air quality in such a way that there exists a clear causal relationship between the specific event(s) and the monitored exceedance(s) or violation(s), is not reasonably controllable or preventable, is an event(s) caused by human activity that is unlikely to recur at a particular location or a natural event(s), and is determined by the Administrator in accordance with 40 CFR 50.14 to be an exceptional event.

40 CFR 50.14(c)(1)(i) requires that air agencies must “notify the public promptly whenever an event occurs or is reasonably anticipated to occur which may result in the exceedance of an applicable air quality standard” in accordance with the mitigation requirement at 40 CFR 51.930(a)(1). Details on DES’s public notification can be found in Appendix B.

As specified in 40 CFR 50.14(c)(3)(iv), the following elements must be included to justify the exclusion of air quality data from a NAAQS determination:

1. A narrative conceptual model that describes the event(s) causing the exceedance or violation and a discussion of how emissions from the event(s) led to the exceedance or violation at the affected monitor(s).
2. A demonstration that the event affected air quality in such a way that there exists a clear causal relationship between the specific event and the monitored exceedance or violation.
3. Analyses comparing the claimed event-influenced concentration(s) to concentrations at the same monitoring site at other times. However, the EPA Administrator is restricted from requiring a state to prove a specific percentile point in the distribution of data.
4. A demonstration that the event was both not reasonably controllable and not reasonably preventable.
5. A demonstration that the event was a human activity that is unlikely to recur at a particular location, or was a natural event.

“EPA Guidance on the Preparation of Exceptional Events Demonstration for Wildfire Events that May Influence Ozone Concentrations” (EPA 2016) describes a three-tier analysis approach to determine a “clear causal relationship” for exceptional events, which is summarized below. Section 4 of this document, “Clear Causal Relationship,” provides the details of these analyses.

Tier 1:

Key factors for this tier are exceedances out of the normal ozone season and/or concentrations that are 5–10 ppb greater than non-event-related concentrations.

Tier 2:

There are two key factors for this tier: fire emissions & distance (Q/d) and comparison of event ozone concentrations to non-event high-ozone concentrations. Q/d analysis for August 6, the day with the highest smoke impact in 2018: Even with the contribution from the three largest and two smaller wildfires, the Q/d threshold could not be achieved due to the significant distance between Las Vegas and the wildfires’ origin points. Since even the worst-case event failed to meet the Q/d threshold, it seemed pointless to perform this analysis for other, lesser wildfire events.

This tier may include additional analyses of smoke maps, plume trajectories, satellite retrievals, sounding data, and time series of supporting ground measurements to provide evidence of wildfire emissions transported to local monitors.

Tier 3:

This tier involves statistical modeling of MDA8 ozone concentrations using generalized additive models (GAMs) to assess wildfire influences on local ozone concentrations.

DES has prepared this package to meet the requirements for seeking EPA concurrence for data exclusion.

This exceptional event demonstration will undergo a 30-day public comment period concurrent with EPA’s review beginning September 3, 2021. A copy of the public notice, along with any comments received and responses to those comments, will be submitted to EPA after the comment period has closed, consistent with the requirements of 40 CFR 50.14(c)(3)(v). Appendix C documents the public comment process.

1.3 REGULATORY SIGNIFICANCE OF THE EXCLUSION

The LVV, located within Clark County, Nevada, is currently designated as a nonattainment area for the 2015 ozone NAAQS of 70 ppb. Table 1-2 lists the 4th highest 8-hour average ozone recorded at the monitors listed in Table 1-1—including wildfire days in 2018 and excluding wildfire days in 2020—for the most recent three-year period (2018–2020), along with the resulting design value (DV) for each monitor. The table also shows the 4th highest 8-hour average ozone and DVs for 2018 after the requested exceedance days are excluded from the DV calculation (the shaded columns). Since the recalculated DVs meet the 2015 NAAQS, the valley would be reclassified as “attainment” if EPA concurs with this demonstration. EPA concurrence will thus have a significant impact on DES’s attainment of the 2015 ozone NAAQS.

Table 1-2. Impact of Wildfire Events on Design Values of 2018–2020 (all values in ppb)

| Site Name | Fourth Highest Average | | | Current | Wildfire Days Excluded | |
|----------------|------------------------|------|-------------------|--------------|------------------------|--------------|
| | 2018 | 2019 | 2020 ¹ | Design Value | 2018 | Design Value |
| Jerome Mack | 75 | 66 | 67 | 69 | 72 | 68 |
| Paul Meyer | 75 | 69 | 70 | 71 | 71 | 70 |
| Joe Neal | 76 | 68 | 68 | 70 | 71 | 69 |
| Walter Johnson | 76 | 68 | 70 | 71 | 73 | 70 |
| Palo Verde | 72 | 62 | 67 | 67 | 68 | 65 |
| Green Valley | 77 | 70 | 68 | 71 | 72 | 70 |

¹ Assume wildfire days are excluded.

2.0 AREA DESCRIPTION AND CHARACTERISTICS OF NON-EVENT OZONE FORMATION

2.1 AREA DESCRIPTION

Clark County covers 8,091 square miles at the southern tip of Nevada and has a population of over 2.2 million.¹ More than 95% of the county’s residents live in the Las Vegas Valley, which is part of the Mojave Desert and constitutes Hydrographic Area (HA) 212. The valley encompasses about 1,600 km² and is surrounded by mountains extending 2,000–10,000 feet above its floor (Figure 2-1). The valley slopes downward from west to east (approximately 900 to 500 m above mean sea level), which affects the local climatology by driving variations in wind, temperature, and precipitation.

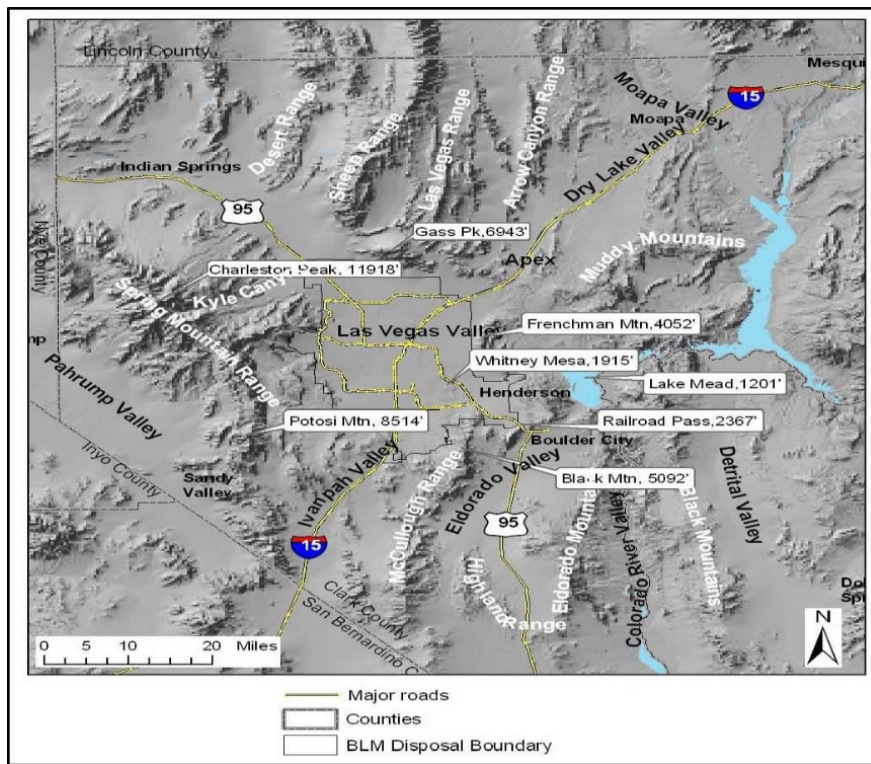


Figure 2-1. Mountain Ranges and Hydrographic Areas Surrounding the Las Vegas Valley.

Valley weather is characterized by low rainfall, hot summers, and mild winters. On average, June is the driest month; monsoons from the Gulf of California increase the humidity and cloud cover in July and August. The Interstate 15 (I-15) corridor through the Mojave Desert and Cajon Pass links Las Vegas with the eastern Los Angeles Basin, about 275 km to the southwest. This corridor is a potential pathway for the export of pollution from Los Angeles to the Mojave Desert and the LVV.

¹ Clark County, Nevada 2017 Population Estimates. Clark County (NV) Department of Comprehensive Planning.

Figure 2-2 shows the locations of Clark County ozone monitors. Most of the stations—Paul Meyer (PM), Walter Johnson (WJ), Palo Verde (PV), Joe Neal (JO), Jerome Mack (JM), and Green Valley (GV)—are in the populated areas of the valley (HA 212), but there are outlying stations in Apex, Mesquite, Boulder City, Jean, and Indian Springs. A station at the Spring Mountain Youth Camp was operated as a special purpose monitoring site for part of the 2018 ozone season.

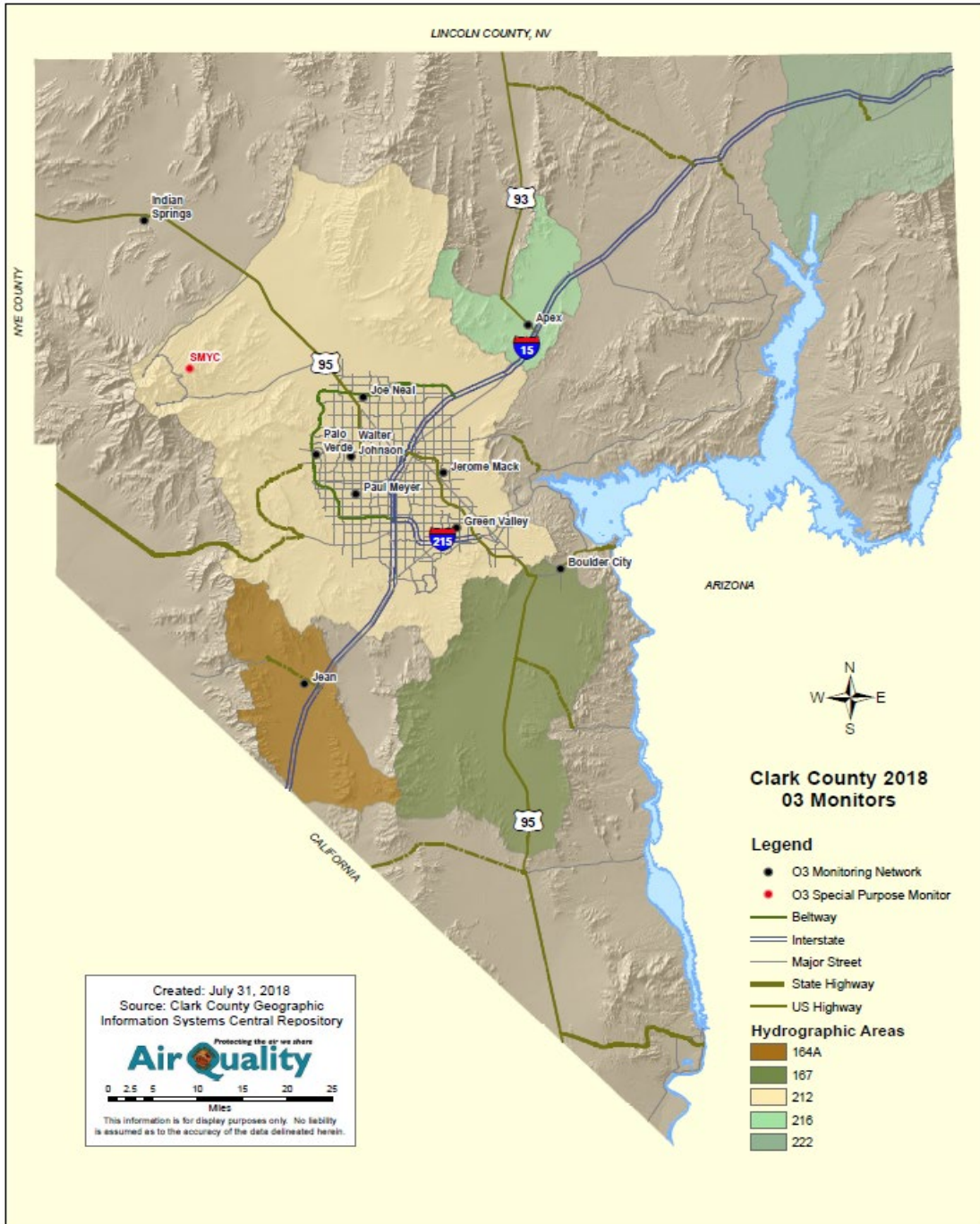


Figure 2-2. Clark County O₃ Monitoring Network.

Figures 2-3 and 2-4 show the locations of Clark County’s Federal Equivalent Method (FEM) and Federal Reference Method (FRM) PM_{2.5} monitors, respectively. Most of the stations are located in the populated areas of HA 212, with one outlying station in Jean, Nevada. Jean is considered a regional background site because it is located far enough from the valley to avoid impacts from local emissions. It is upwind of the LVV, but downwind of southern California.

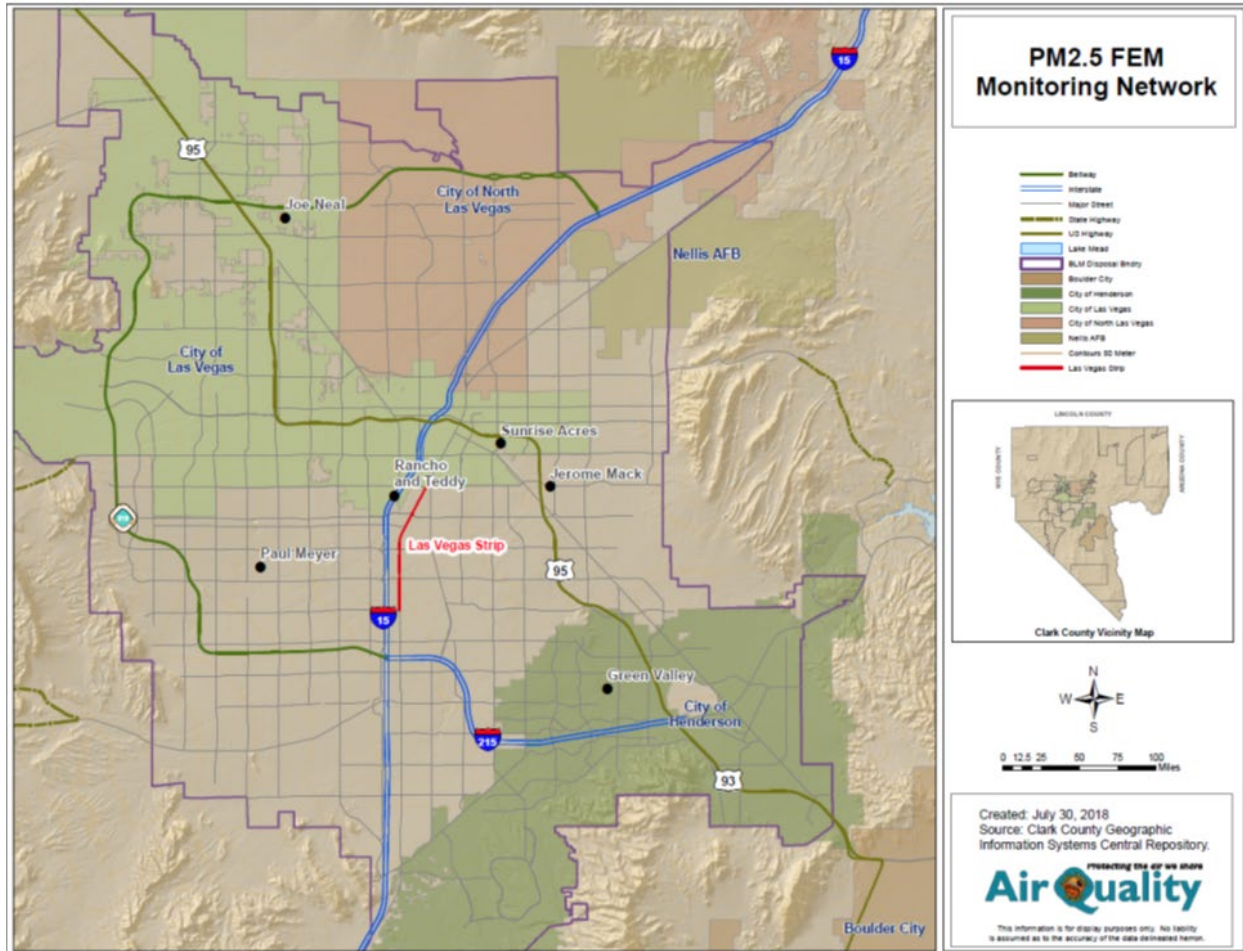


Figure 2-3. Locations of FEM PM_{2.5} Monitors.

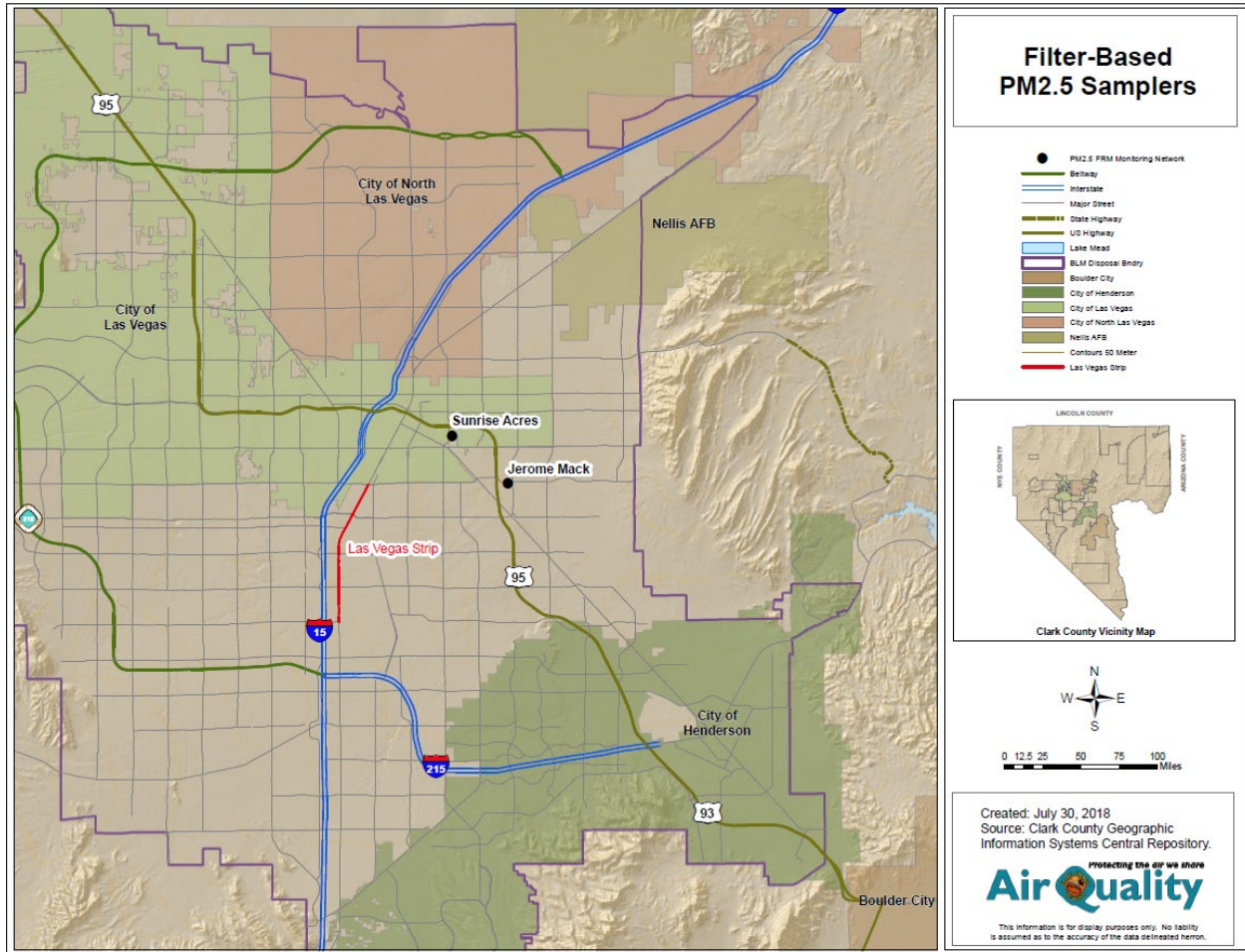


Figure 2-4. Locations of FRM PM_{2.5} Monitors.

2.2 CHARACTERISTICS OF NON-EVENT OZONE FORMATION

Ozone, a secondary pollutant, is formed by complex processes in the interaction of nitrogen oxides (NO_x), volatile organic compounds (VOCs), temperature, and the intensity of solar radiation. The elevated ozone in the LVV can be characterized as the result of a combination of locally produced ozone under relatively stagnant conditions and different degrees of regional transport from upwind source areas, mainly in California.

2.2.1 Emission Trend

Mobile emission is the largest source of ozone precursors in Clark County. The area adjacent to two major transportation routes, I-15 and U.S. Highway 95, registers the highest emissions in the LVV. Figures 2-5 and 2-6 illustrate the county's ozone planning inventory for NO_x and VOC emissions, respectively, on a typical summer weekday. Throughout the years, ozone has decreased dramatically across much of the eastern United States over the last two decades (He et al.

2013; Lefohn et al. 2010), largely as a result of stricter emission controls on stationary and mobile NO_x sources (Butler et al. 2011; EPA 2012). These same reductions can be seen in California and Clark County.

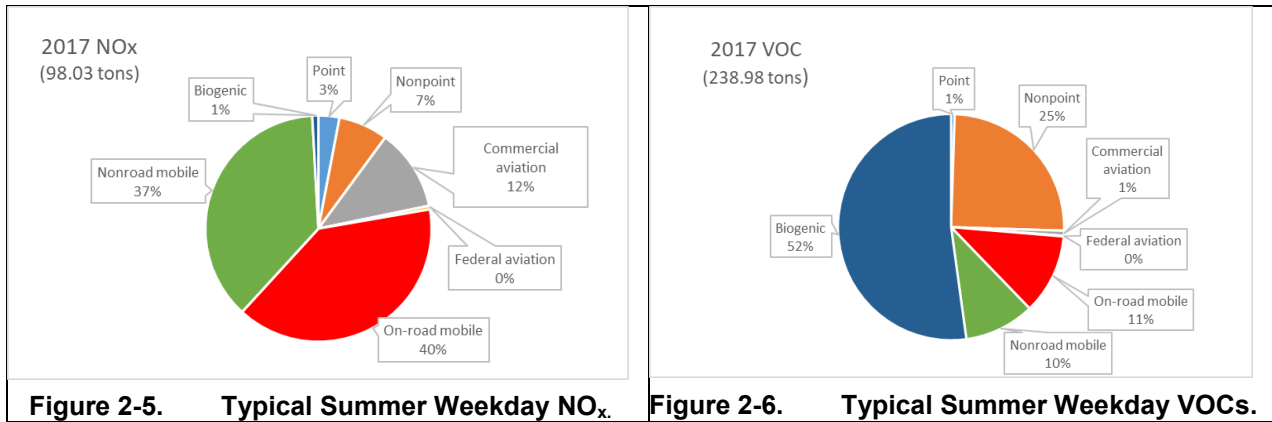
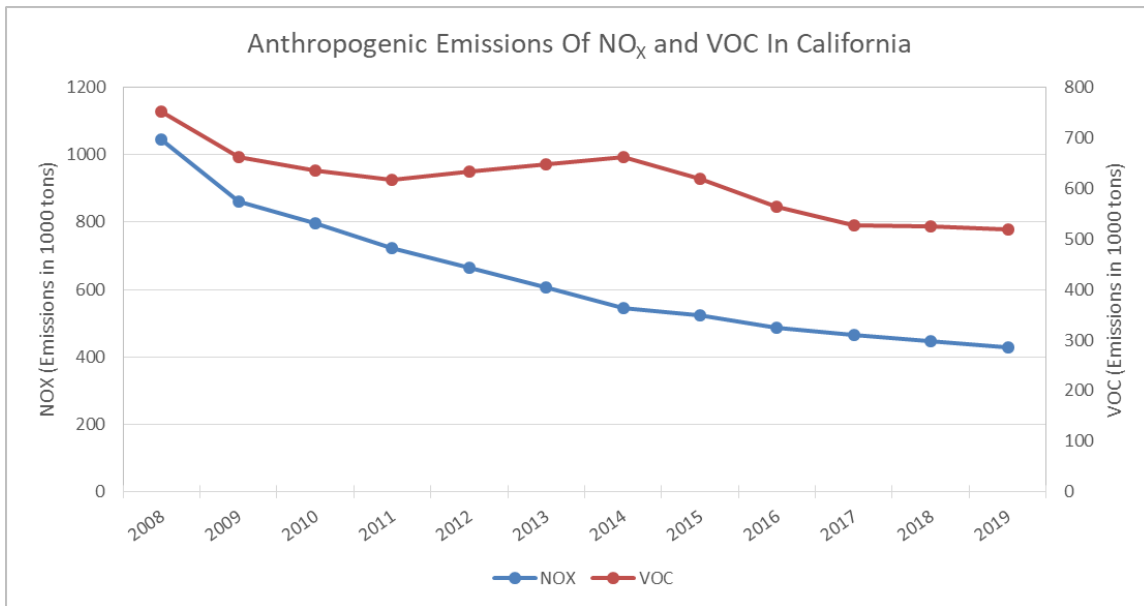


Figure 2-5. Typical Summer Weekday NO_x. **Figure 2-6. Typical Summer Weekday VOCs.**
 Source: https://www.clarkcountynv.gov/Environmental%20Sustainability/SIP%20Related%20Documents/O3/20200901_2015_O3_EI_ES_SIP_with_Appendices.pdf?t=1619706653363.

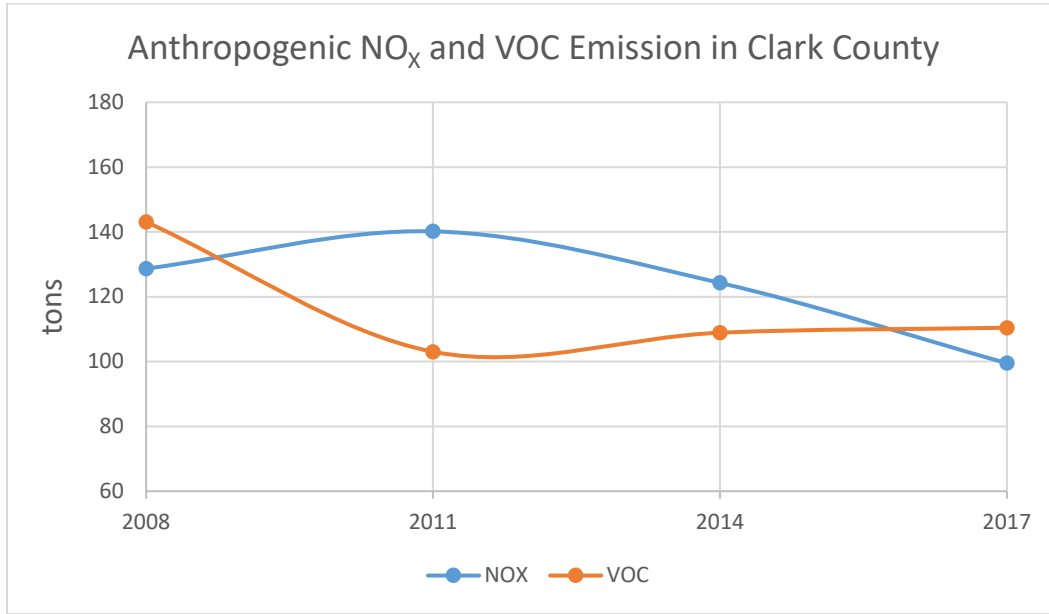
Figure 2-7 shows the downward trends of NO_x and VOC anthropogenic emissions in California from 1990–2019.



Source: <https://www.epa.gov/air-emissions-inventories/air-pollutant-emissions-trends-data> (under State Annual Emissions Trend).

Figure 2-7. Anthropogenic Emission Trends of NO_x and VOC in California, 2008–2019.

Figure 2-8 shows a downward trend in NO_x emissions and a slight increase in VOC anthropogenic emissions in Clark County from 2008–2017.



Source: <https://www.epa.gov/air-emissions-inventories/national-emissions-inventory-nei>.

Figure 2-8. Anthropogenic Emission Trends of NO_x and VOCs in Clark County, 2008–2017.

After a substantial reduction in NO_x emissions (approximately 55% in California and 25% locally) over the past 10 years, Figure 2-9 illustrates how the eight-hour ozone 4th highest averages in Clark County generally trended downward from 2009–2019 (except in 2018).

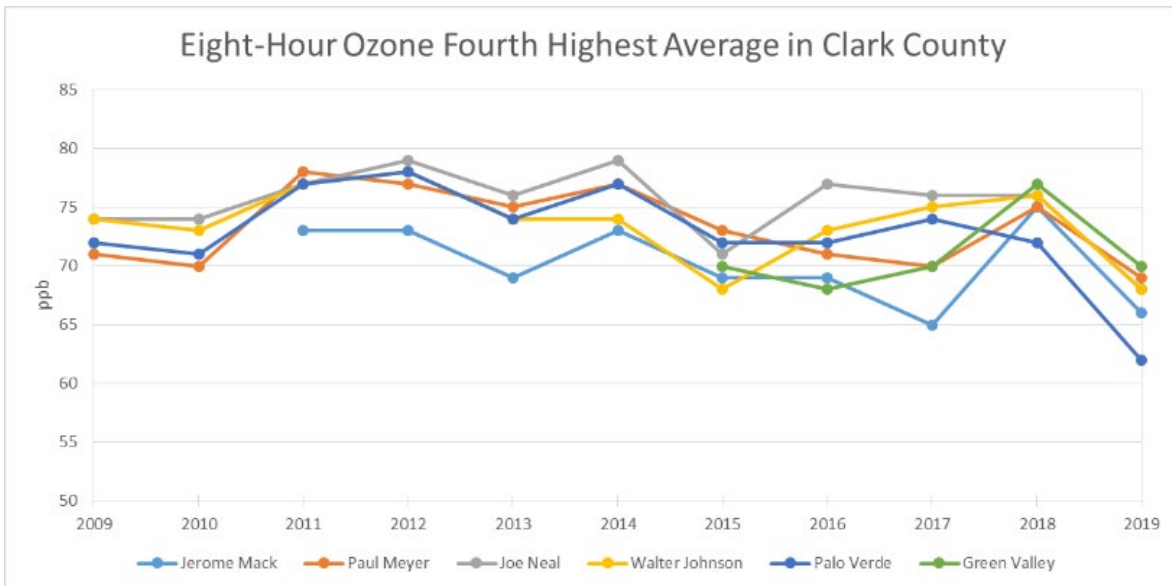


Figure 2-9. Eight-hour Ozone 4th Highest Average at Monitors in Clark County, 2009–2019.

2.2.2 Weather Patterns Leading to Ozone Formation

Most of the high ozone days in the Las Vegas Valley occur from May through August. During these months, warmer temperatures lead to the development of regional-scale southwest-northeast plains-mountain circulations and locally-driven valley and slope flows (Stewart et al. 2002). In general, winds during the nocturnal regime are dominated by downslope flows from the east and southwest converging into Las Vegas; downslope flows have also been observed northeast of the Spring Mountain Range. Southeasterly to southerly wind flow develops during the morning transition period, but the winds shift to the southwest by mid-afternoon as the mixed layer grows in depth and plains-mountain winds develop, driven by the thermal contrast between the land and the Gulf of California. This regional-scale flow converges with southeasterly up-valley flow in the LVV, and these winds typically persist until well into the night, when the nocturnal regime prevails again.

The convergence of afternoon southwesterly plain-mountain and southeasterly up-valley flows at the northwestern terminus of the valley frequently results in elevated ozone levels at JO and WJ. Figure 2-10 illustrates the typical ozone season (May–August) diurnal ozone patterns at the 50th and 95th percentiles at all monitors in HA 212. These patterns are based on historic ozone data from 2014–2018.

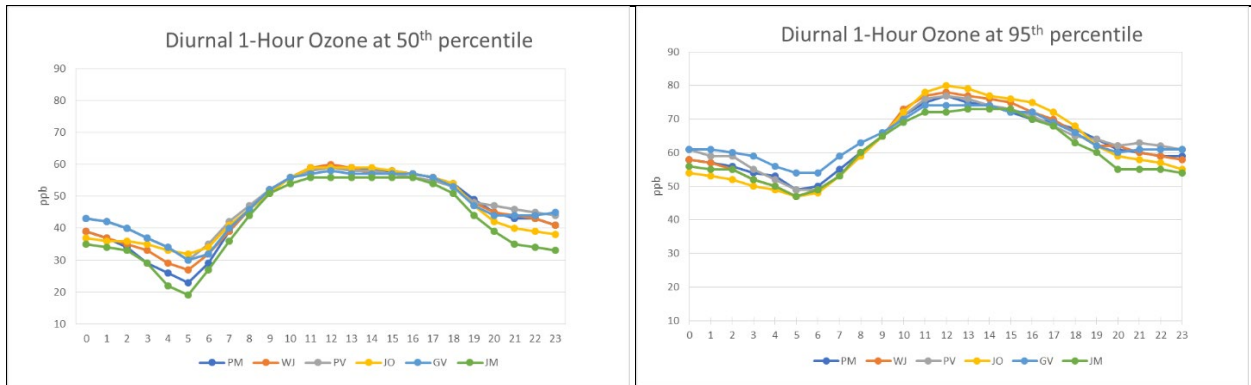
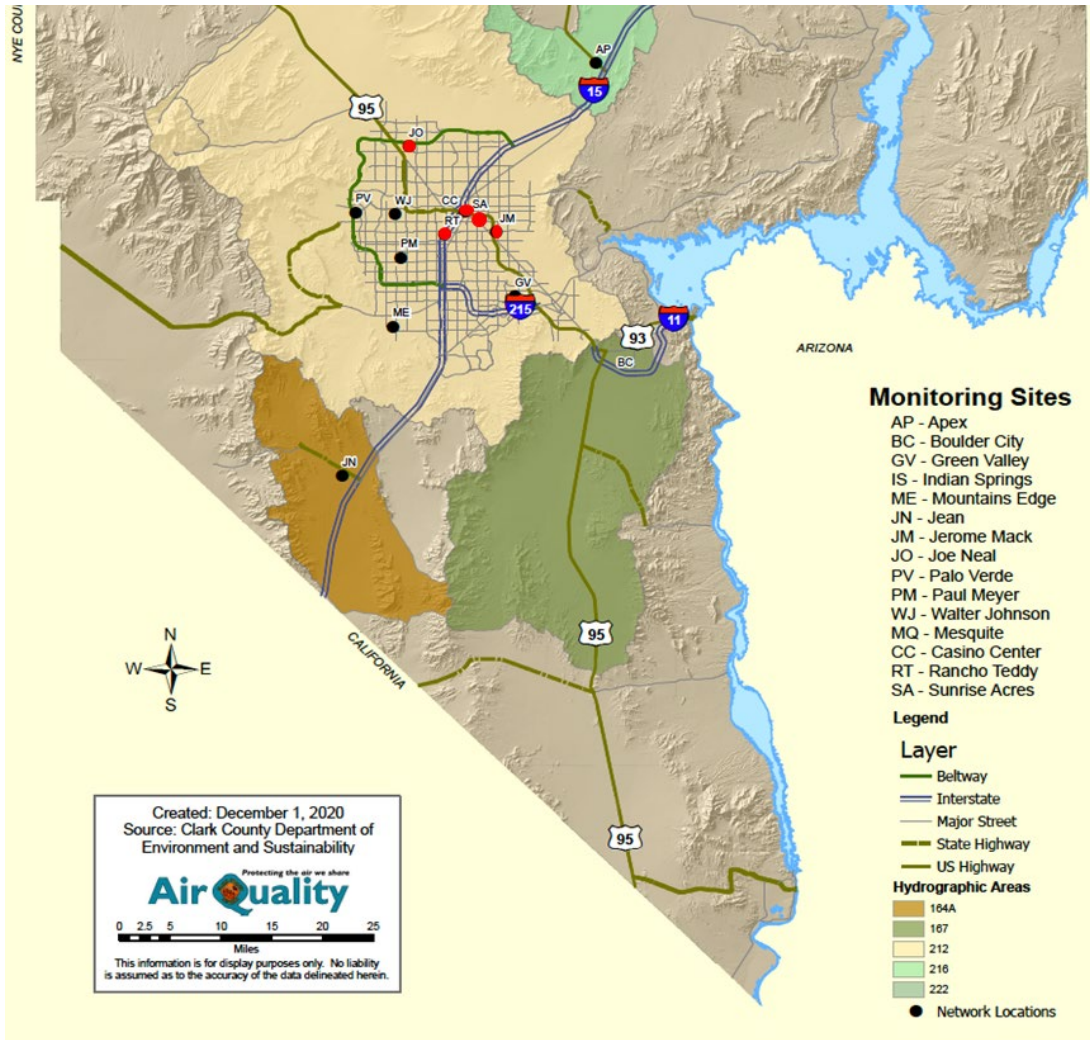


Figure 2-10. Typical Ozone Season 1-Hour Ozone Diurnal Pattern for 50th and 95th Percentile Values at Clark County Monitors.

2.2.3 Weekday and Weekend Effect

Figure 2-11 depicts air quality monitors in the LVV; the NO₂ monitors at Rancho Teddy (RT), Casino Center (CC), Sunrise Acres (SA), JM, and JO are marked as red dots. Most anthropogenic precursors are emitted from the urban core and follow a diurnal pattern related to traffic patterns, which peak twice daily at the morning and evening rush hours (Figure 2-12).



Note: Red dots = NO₂ monitors.

Figure 2-11. Locations of NO₂ Monitors.

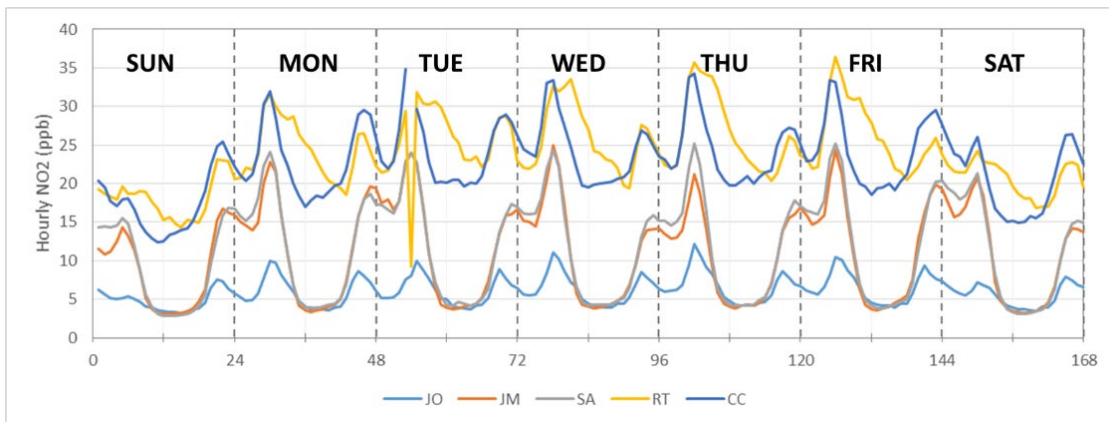


Figure 2-12. Weekly Pattern for 1-Hour NO₂ at Monitors from 2014–2019 (May-August).

Figure 2-13 shows that daily average NO₂ concentrations are lower on weekends than weekdays. The highest NO₂ concentrations are at RT and CC (urban core-downtown), and the lowest are at JO (further downwind). These weekly patterns are based on historic hourly and daily NO₂ concentrations recorded between 2014 and 2019 (May–August).

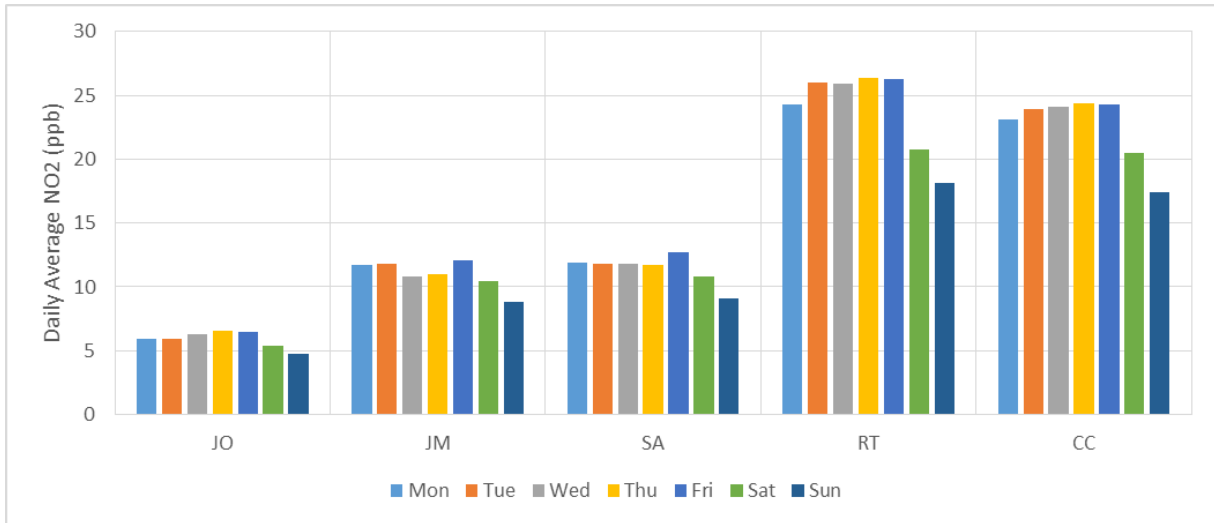


Figure 2-13. Weekly Pattern for 24-Hour NO₂ average at Monitors from 2014–2019 (May–August).

Figure 2-14 shows the mean MDA8 O₃ at six monitors in HA 212 (see Figure 2-2) and the up-wind monitor at Jean. It shows these sites have a similar weekly pattern, with the highest MDA8 O₃ on Fridays and Saturdays despite significantly lower concentrations of NO₂ (an O₃ precursor) on Saturdays (Figure 2-13). It also indicates MDA8 O₃ at those sites differs minimally between weekdays and weekends, with a maximum difference of 1.7~2.4 ppb. The data in this analysis are based on historic O₃ concentrations recorded between 2014 and 2019 (May–August).

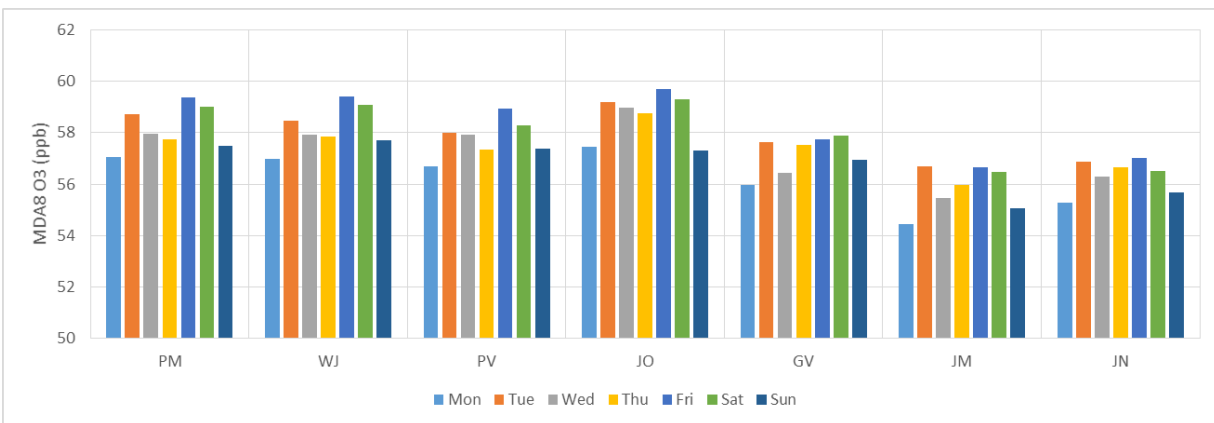


Figure 2-14. Weekly Pattern for MDA8 O₃ Average at Monitors, 2014–2019 (May–August).

3.0 EVENT SUMMARY AND CONCEPTUAL MODEL

3.1 PREVIOUS RESEARCH ON OZONE FORMATION AND SMOKE IMPACTS

The impact of wildfires on ozone concentrations at both local and regional levels has been studied extensively. Nikolov (2008) provides an excellent summary of past studies, as well as a conceptual discussion of the physical and chemical mechanisms contributing to observed impacts. Nikolov concludes that on a regional scale, biomass burning can significantly increase background surface ozone concentrations, resulting in NAAQS exceedances. Pfister et al. (2008) simulated the large fires of 2007 in northern and southern California; the authors found ozone increases of approximately 15 ppb in many locations and concluded, “Our findings demonstrate a clear impact of wildfires on surface ozone nearby and potentially far downwind from the fire location, and show that intense wildfire periods frequently can cause ozone levels to exceed current health standards.” In a presentation at an emission inventory conference, Pace et al. (2007) modeled the June 2005 California fires, showing that the wildfire impacts added as much as 15 ppb to ozone concentrations in southern Nevada (Figure 3-1).

Finally, in one of DES’s own studies (DES 2008), aircraft flights through smoke plumes demonstrated increased ozone concentrations of 15 to 30 ppb in California. Two other field campaign studies (DES 2013 & 2017) conducted by National Oceanic and Atmospheric Administration (NOAA) scientists have shown that large fires in California could have adversely impacted the air quality in Clark County.

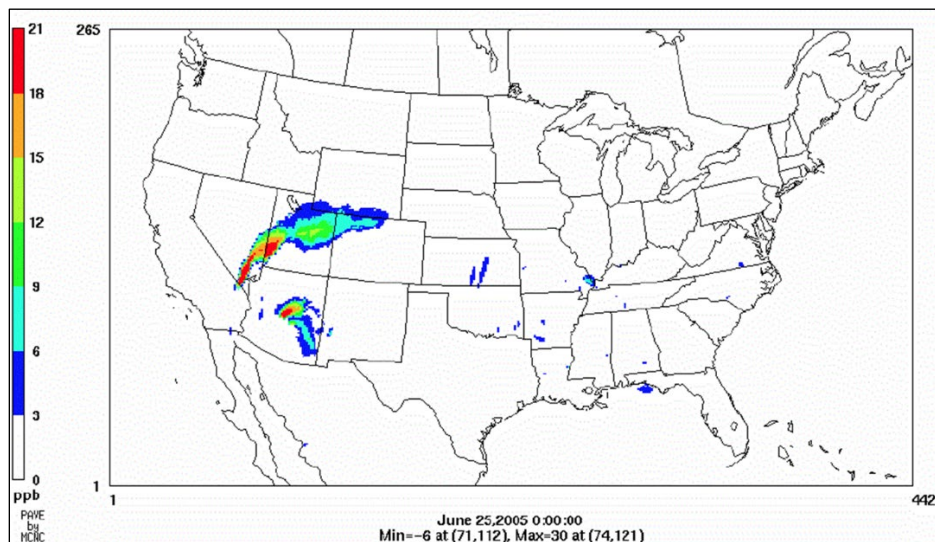
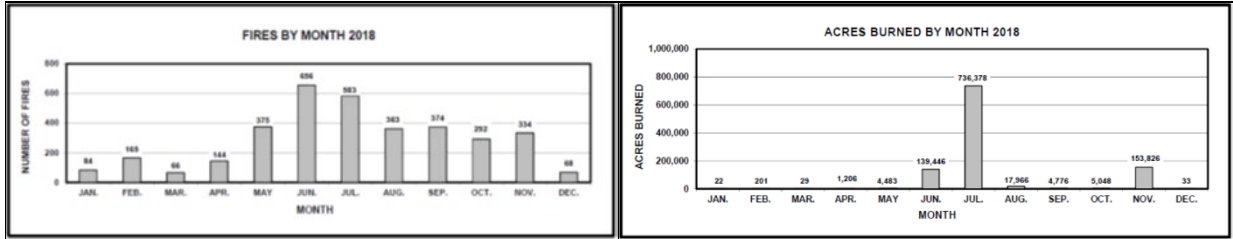


Figure 3-1. Difference (“Fire” / “No Fire”) in Maximum 8-hour Ozone for June 25, 2005.

3.2 CALIFORNIA WILDFIRES IN 2018

Wildfires in the western states are worsening every year: they are bigger, hotter, more deadly, and more destructive. In California in 2018, the combination of natural fuel from a record 129 million trees killed by drought and bark beetles (as reported by the United States Forest Service) and compounding atmospheric conditions led to numerous large and small wildfires. The number

of fires and burned area increased greatly in June and July, as shown in Figure 3-2. Significant wildfires started breaking out in June of that year; later in the summer, a series of large wildfires erupted across California, mostly in the northern part of the state, including the destructive Carr and Mendocino Complex Fires. Figure 3-3 shows the more frequent ozone exceedances in the LVV after mid-June, reflecting the impact of the California wildfires during this period.



Source: CAL FIRE 2018 Wildfire Activity Statistics Report.

Figure 3-2. Number of Fires and Acres Burned by Month.

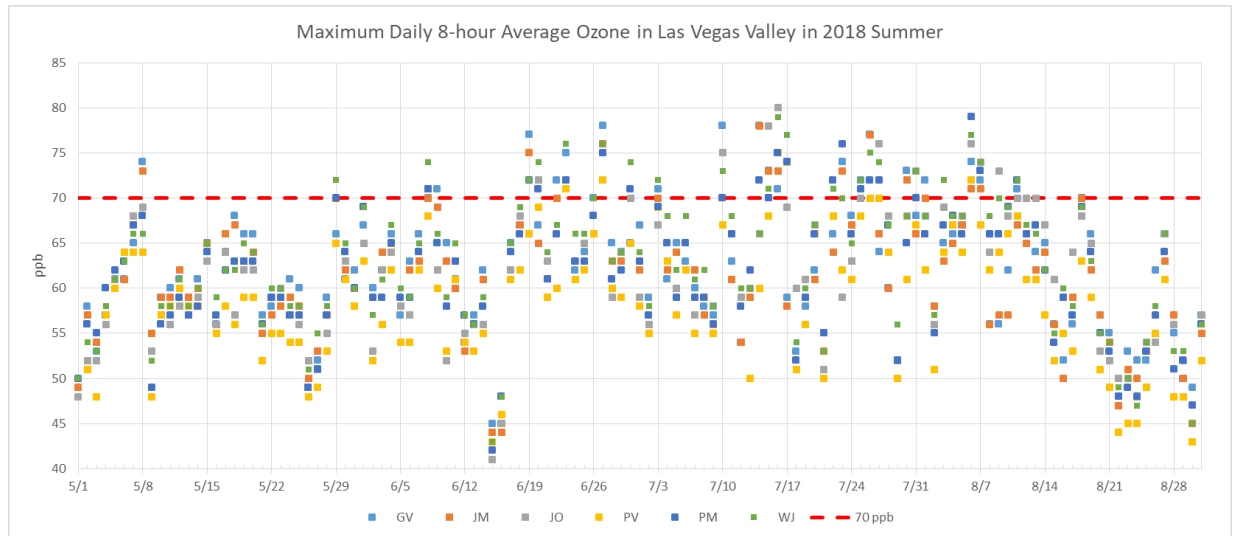


Figure 3-3. MDA8 Ozone Levels at LVV Monitors during 2018 Ozone Season.

3.3 JUNE 27, 2018

Hundreds of lightning strikes on June 20 and 21 caused nearly 70 wildfires throughout central Oregon, three (Jack Knife, Boxcar, and Graham) classified as major. Although they were huge wildfires, their influence was minimal because of a relatively long distance; however, two large fires that broke out on June 23, Pawnee and Lane, and the reigniting Lions Fire influenced ozone concentrations in the LVV on June 27. Figure 3-4 shows the fire locations and smoke plumes from Oregon and northern/central California being transported towards the southern California desert and southern Nevada on June 24 and 25. The Pawnee Fire burned a total of 15,185 acres before it was contained on July 8, 2018; the Lane Fire burned a total of 3,716 acres before it was contained on July 4, 2018.

The Lions Fire started in the Sierra National Forest around June 1 as a lightning strike, burning near the Lion Point area in the Ansel Adams Wilderness. It crossed into the Inyo National Forest on June 22 and spread to the south and west on June 24, with a total of 1,000 acres burned (<https://www.fs.usda.gov/detail/sierra/news-events/?cid=FSEPRD585182>). Strong winds expanded a reigniting Lions Fire to 2,382 acres by June 24. More small fires broke out in northern and central California between June 23 and 26; on June 25, fires at the Mexico/California border increased in intensity. During this period, weather patterns transported the wildfire smoke to the desert area in southern California between Las Vegas and Mexico.

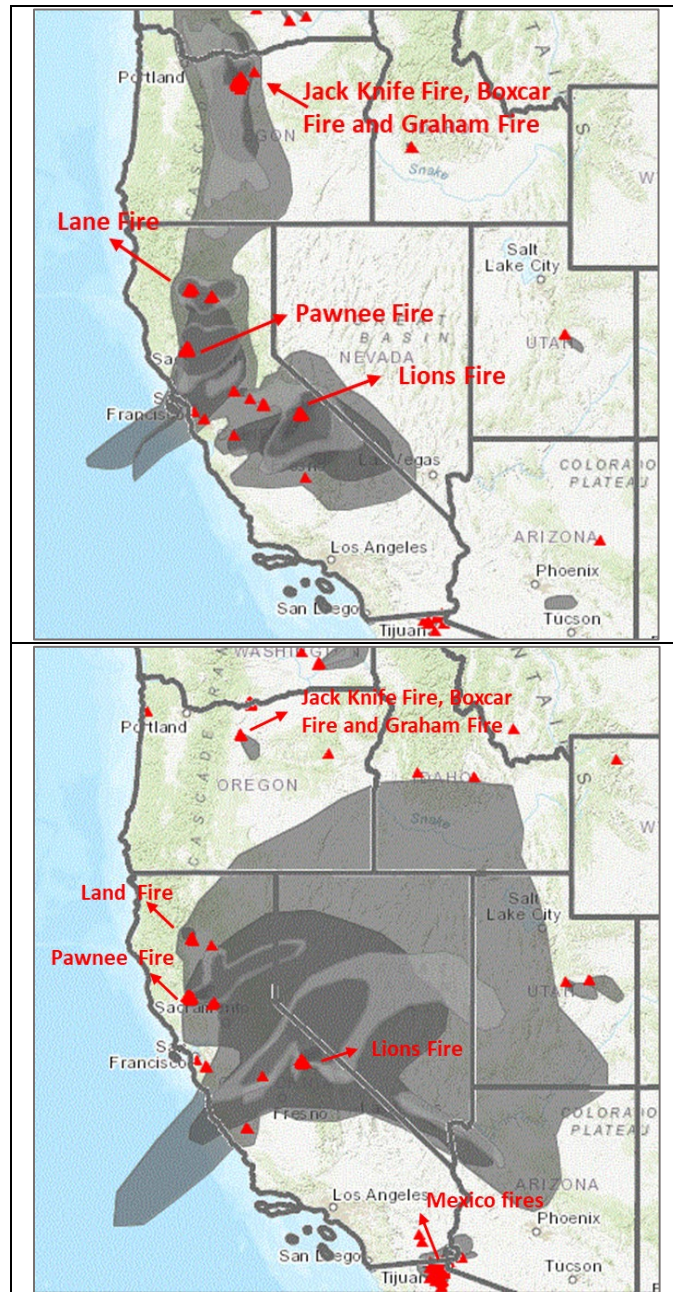


Figure 3-4. NOAA Daily Hazard Mapping System Smoke Analysis on June 24 (top) and June 25 (bottom).

An examination of the synoptic weather patterns at the 500-mb level from June 24–27 (Figure 3-5) shows a low pressure system west of the Canadian coast moving slowly eastward to east Alberta, and a high pressure system moving north toward the higher-latitude region in the U.S. On June 24, the low pressure system provided a northwest-northerly wind over the West Coast, pushing smoke southeastward, as shown in the NOAA Hazard Mapping System smoke analysis (Figure 3-4). The next day, the edge of a cold front on surface map in Figure 3-6 moved through northern California and continued moving east. Behind the cold front, the smoke subsided to the surface and merged with smoke from other wildfires in California under the high pressure system dominating the southwestern U.S. The persistent high pressure for June 25–27 created weather conditions of low wind speeds and weak valley ventilation in the LVV. At the same time this trough was sitting over the surface of southern Nevada, 850-mb maps of June 25–27 (Figure 3-7) show wind generally blowing northwesterly from a wildfire in Mexico toward the California deserts. On June 26–27, the warmest temperature area on the 850-mb maps was over Clark County and the skew-T diagram (Figure 3-8) show both days had deep and neutrally stratified nocturnal residual layer. They indicate that substantial stability and capping (i.e., temperature inversion) was occurring on those days; this lingering transported smoke trapped in the LVV, paired with meteorological conditions favoring ozone formation (Figure 3-9), contributed to ozone exceedances at all monitors (72~78 ppb, Table 1-1) in HA 212 on June 27. Figure 3-10 illustrates a simplified conceptual model of the June 27, 2018, wildfire-influenced ozone event.

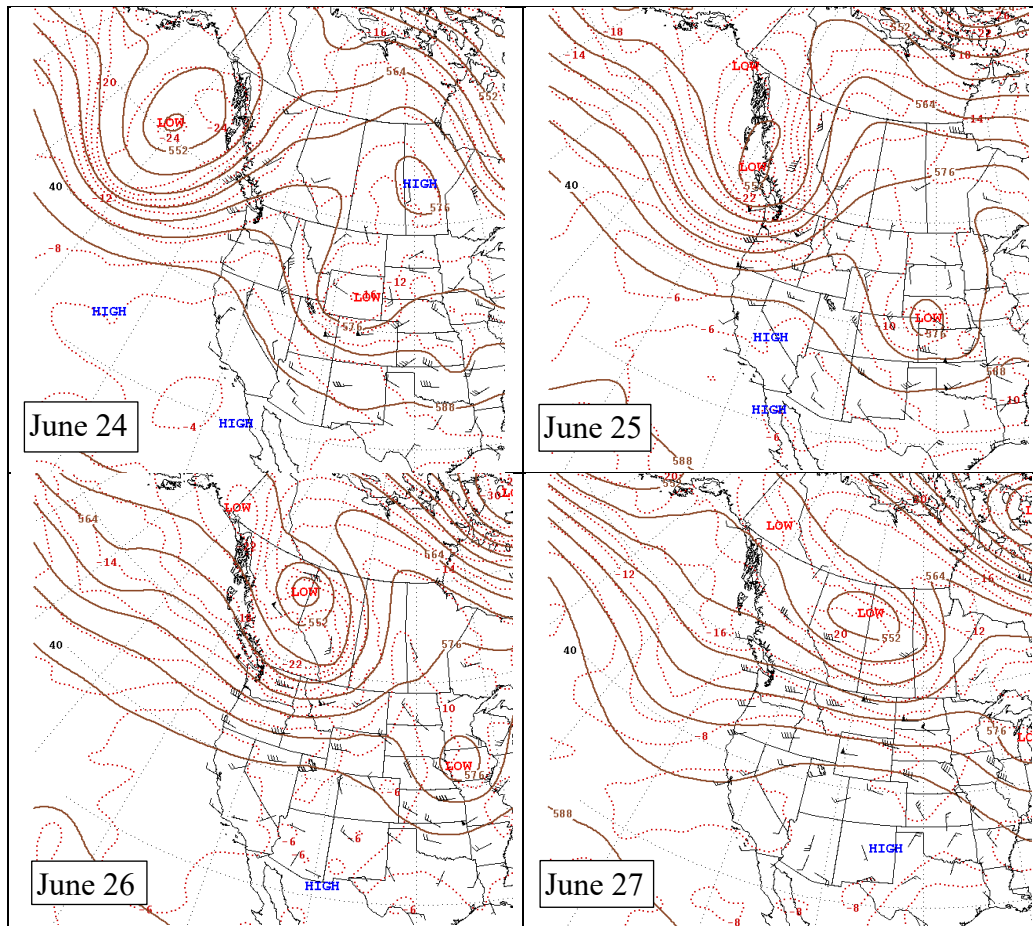


Figure 3-5. 500-mb Weather Patterns at 7 AM EST, June 24–27.

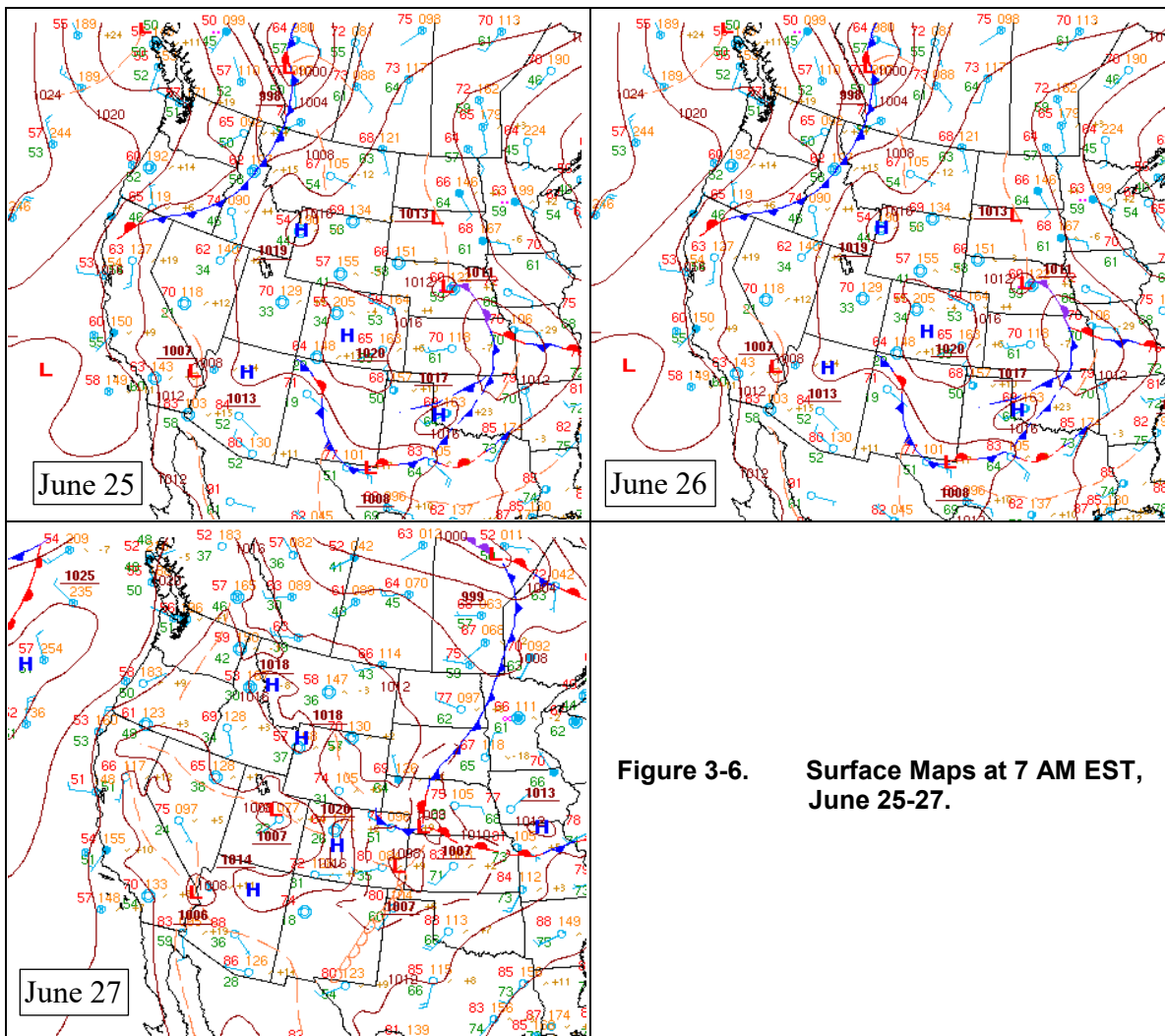


Figure 3-6. Surface Maps at 7 AM EST, June 25-27.

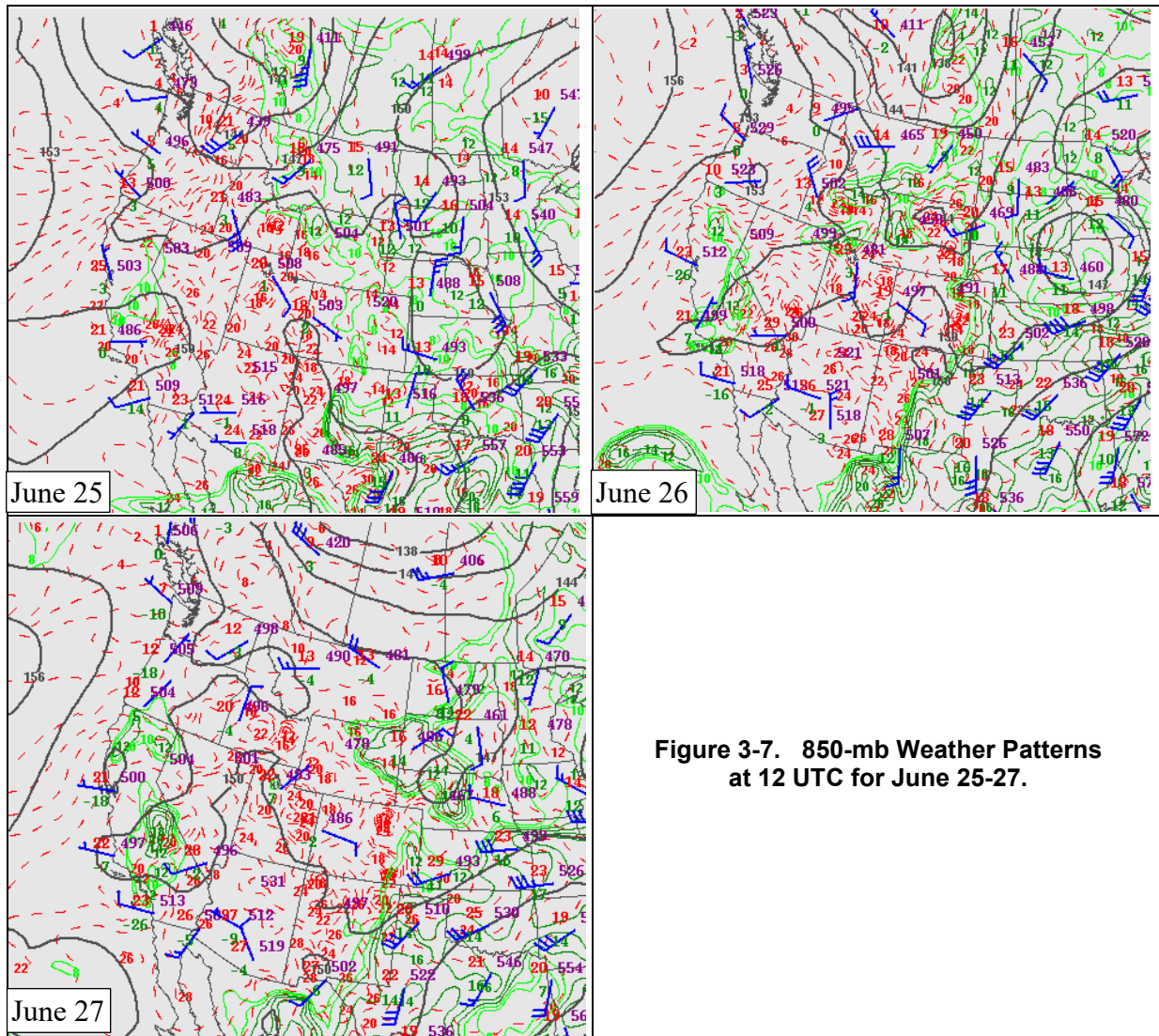
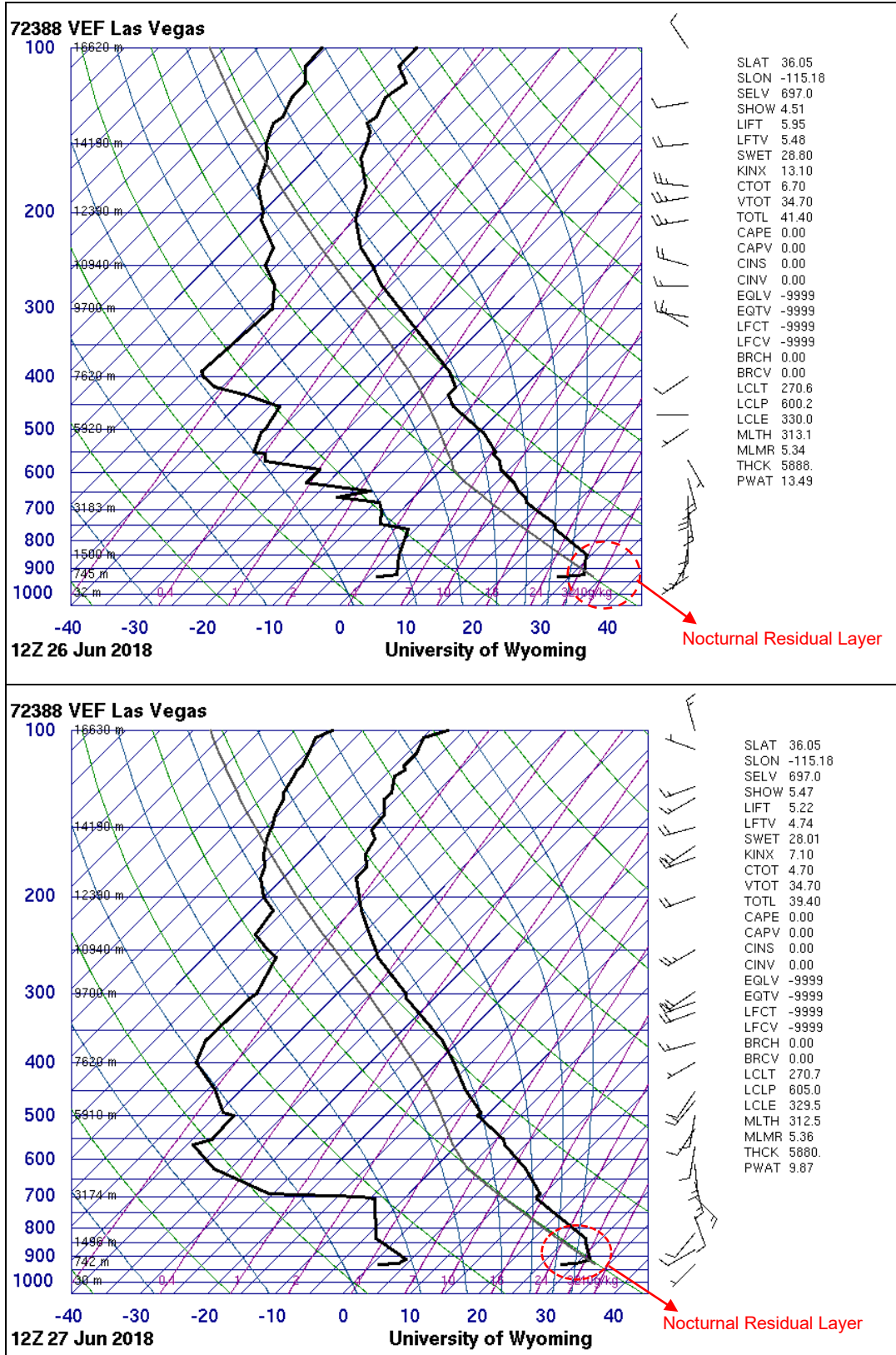
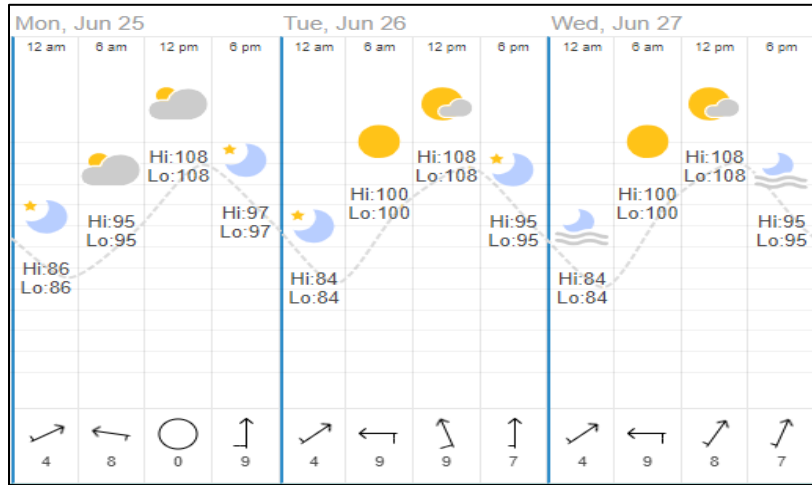


Figure 3-7. 850-mb Weather Patterns at 12 UTC for June 25-27.



Source: <http://weather.uwyo.edu/upperair/sounding.html>

Figure 3-8. Upper LVV Weather: Skew-T diagrams at 12Z on June 26–27.



Source: <https://www.timeanddate.com/weather/usa/las-vegas/historic>

Figure 3-9. Surface LVV Weather, June 25–27.

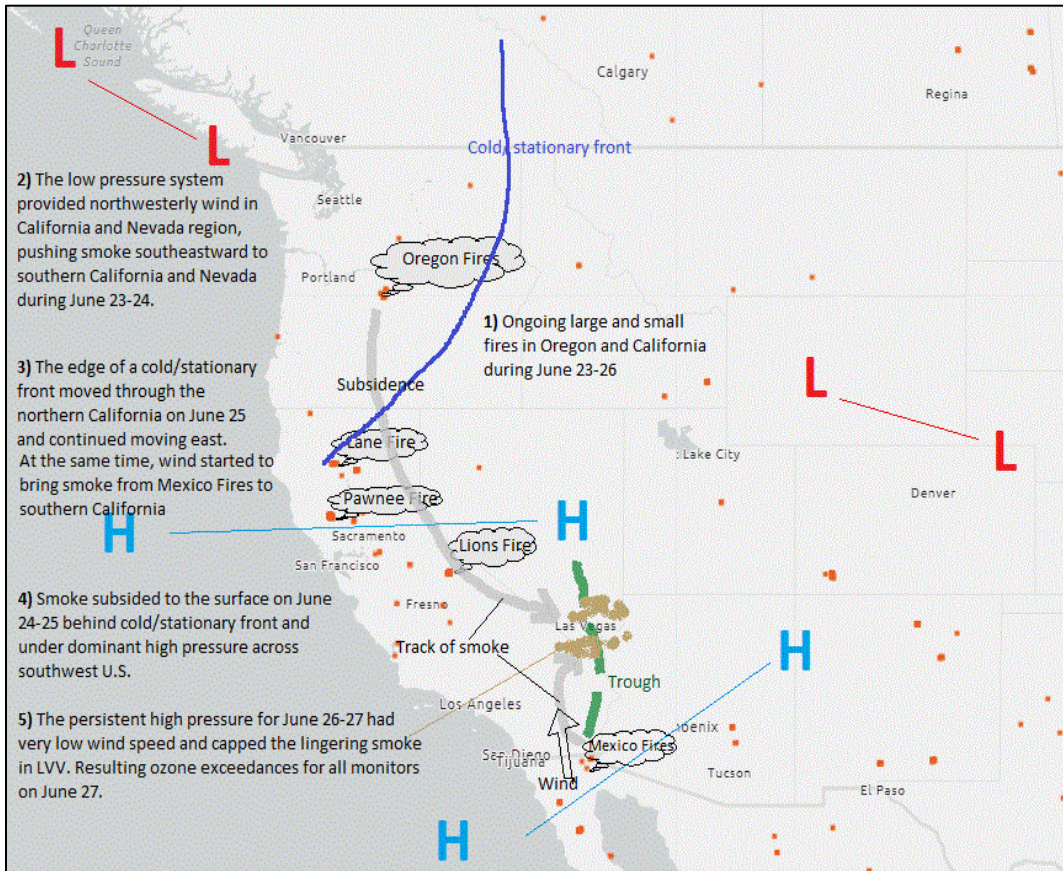


Figure 3-10. Simple Conceptual Model of June 27 Wildfire-Influenced Ozone Event.

4.0 CLEAR CAUSAL RELATIONSHIP

4.1 ANALYSIS APPROACH

Based on EPA's exceptional event guidance, this package provides Tier 1, Tier 2, and Tier 3 analyses to demonstrate a clear causal relationship between the wildfire event and monitored ozone exceedances. The demonstrations in this section provide (1) a comparison of the ozone data requested for exclusion against historical ozone concentrations at the monitor, and (2) a presentation of the path along which fire emissions were transported to the affected monitors.

Tier 1 Analyses

- Event day ozone concentrations are 5–10 ppb higher than non-event-related concentrations (95th percentiles for hourly seasonal ozone for 2014–2018).

Tier 2 Analyses

- Key Factor #1: Q/d analysis (not performed).
- Key Factor #2: Comparison of the event-related MDA8 ozone with historical non-event-related high ozone concentrations (>99th percentile from 2014 to 2018 of MDA8 ozone, or the top four highest daily ozone measurements).
- Visible satellite imagery.
- Hybrid Single-Particle Lagrangian Integrated Trajectory (HYSPLIT) model backward trajectories.
- Satellite data retrieval: Aerosol Optical Depth (AOD) maps.
- Concurrent rise in ozone concentrations.
- Analysis of PM_{2.5} speciation data.
- Analysis of levoglucosan (trace of fire emissions).
- Supporting ground measurements: Event-related diurnal PM_{2.5}, NO₂, and CO (wildfire plume components) concentrations showed elevated concentrations and/or changes in diurnal profile consistent with smoke impacts.

Tier 3 Analyses

- GAM statistical model.

Key Factor #1 for a Tier 2 analysis uses an **emissions divided by distance (Q/d)** relationship to estimate the influence of fire emissions on a downwind monitor. If $Q/d \cdot (\text{daily aggregated fires}) \geq 100$, then the fires satisfy the Q/d test. A Q/d analysis for August 6, the day with the highest smoke impact in 2018, was performed in the concurrent *Exceptional Event Demonstration for Ozone Exceedances in Clark County, Nevada—August 6-7, 2020*. Even using the smoke from the three largest wildfires and other small wildfires in California for the August 6–7, 2018 event, the Q/d threshold could not be achieved due to the significant distance between Las Vegas and the wildfires' origin points. Therefore, this document provides no Q/d analyses for this event.

We examined AOD maps from the Moderate Resolution Imaging Spectroradiometer (MODIS) instruments onboard the National Aeronautics and Space Administration's (NASA's) Aqua and

Terra satellites using the Worldview tool. Since AOD indicates the concentration of aerosols in the total atmospheric column, analyzing AOD maps can help to recognize the movements of smoke.

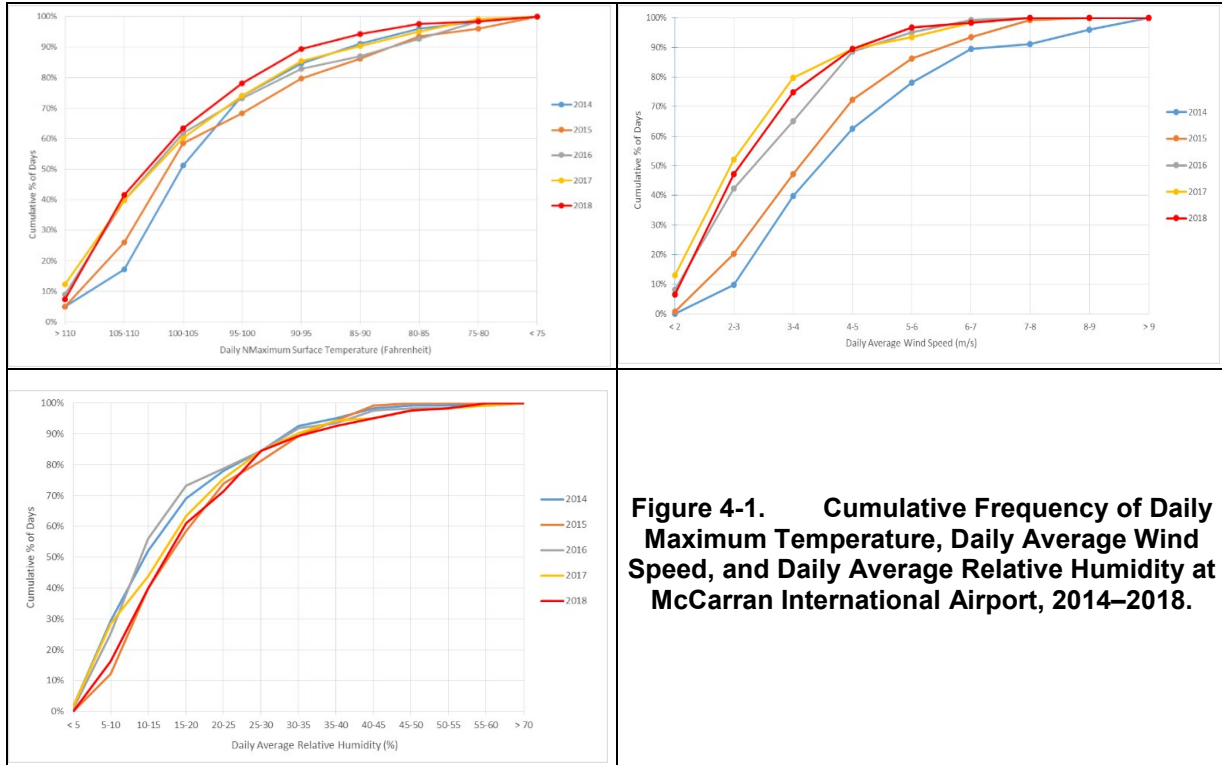
In addition to analysis of PM_{2.5} speciation data, levoglucosan—a unique tracer for burning biomass in PM_{2.5} samples—can serve as a wildfire indicator. Levoglucosan has an atmospheric lifetime of one to four days before it is lost due to atmospheric oxidation, and can therefore be used as a tracer of biomass burning (wildfires) far downwind from its source (Hoffmann et al. 2009; Hennigan et al. 2010; Bhattarai et al. 2019; Lai et al. 2014). During the summer of 2018, DES collected PM_{2.5} samples every three days at the Jerome Mack and Sunrise Acres monitoring stations. Sample analysis—including for levoglucosan, a wildfire marker—was done by the Desert Research Institute (DRI).

A GAM is a type of statistical model that allows the user to predict a response based on the linear and non-linear effects of multiple variables (Wood 2017). A GAM model developed by Sonoma Technology was used to describe the relationship between MDA8 levels of ozone and primary predictors (e.g., prior day's ozone, meteorology, and transport) from 2014–2020. The details for the model's construction and verification are described in Section 3.3.3, “GAM Statistical Modeling,” of *Exceptional Event Demonstration for Ozone Exceedances in Clark County, Nevada—June 22, 2020*. By comparing GAM-predicted ozone values with actual measured ozone concentrations (i.e., residuals), we can determine the effect of outside influences (e.g., wildfires or stratospheric intrusions) on ozone concentrations each day (Jaffe et al. 2004). The GAM model results presented in this document contain MDA8 ozone predictions, residuals, positive 95th percentile values, predicted fire influence, and percentile rank of positive residuals based on EPA guidance (EPA 2016), which were used to estimate wildfire influence under the meteorological conditions recorded at exceeding sites.

4.2 COMPARISON OF EVENT-RELATED CONCENTRATIONS WITH HISTORICAL CONCENTRATIONS

Outside of the transport of ozone and its precursors from California wildfires, elevated ozone levels in the LVV correlate to local weather conditions and home-grown (Figure 2-7) and upwind (Figure 2-8) California emissions. The declining ozone trend in the LVV (Figure 2-9) reflects the reduction of these emissions over the years. However, 2018 was an exceptional year, with more ozone exceedances than any of the prior years from 2014–2017 (Figure 1-1).

In general, warm, dry weather is more conducive to ozone formation than cool, wet weather. High winds tend to disperse pollutants and can dilute ozone concentrations. We examined three meteorological variables—daily maximum surface temperature, daily average wind speed, and daily average relative humidity—at McCarran International Airport during the 2014–2018 summer months to depict the year-to-year variation of local weather conditions (Figure 4-1).



Overall, 2018 had lower wind speeds, slightly higher temperatures, and slightly more moisture compared to previous years. Yet the mean of 2018 MDA8 ozone is between 4.4 and 7.2 ppb higher than other years (Figure 4-2). Compared to 2014–2017, the summer of 2018 had more California wildfires (Figure 1-1) and relatively stagnant weather conditions (Figure 4-1). This increased background ozone levels in the LVV (Figure 4-2), resulting in a higher number of ozone exceedances than in previous years.

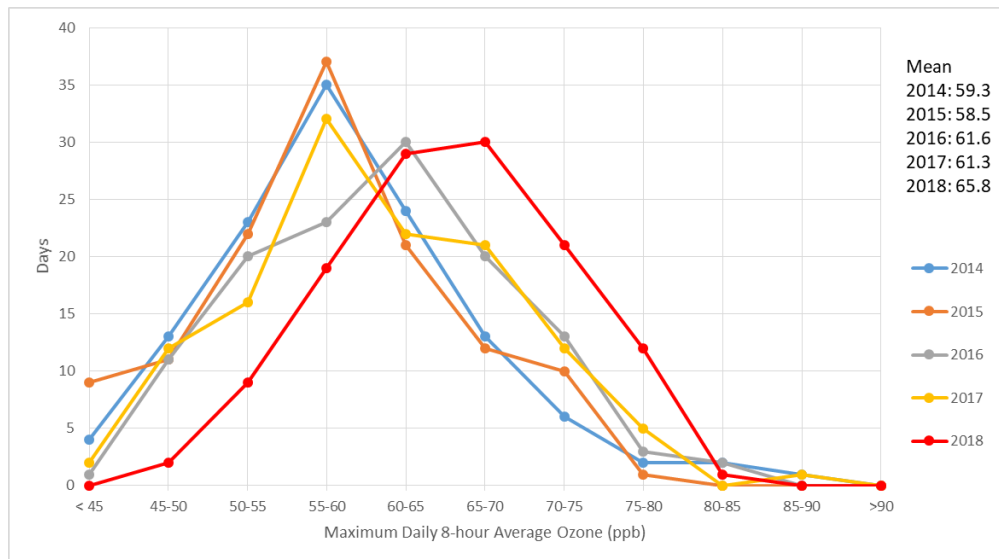


Figure 4-2. Distribution of Days by MDA8 Ozone Levels, 2014–2018.

Figures 4-3 through 4-8 show MDA8 ozone during the 2014–2018 ozone seasons plotted for each monitor against that monitor’s multiseason 95th and 99th percentiles. Red circles indicate the ozone exceedances submitted for the 2018 exceptional events demonstration. All but the following sites and dates exceeded the 95th percentile: Walter Johnson on June 19 and July 15; Palo Verde on July 26 and 27; and Joe Neal on June 20, 23, and 27.

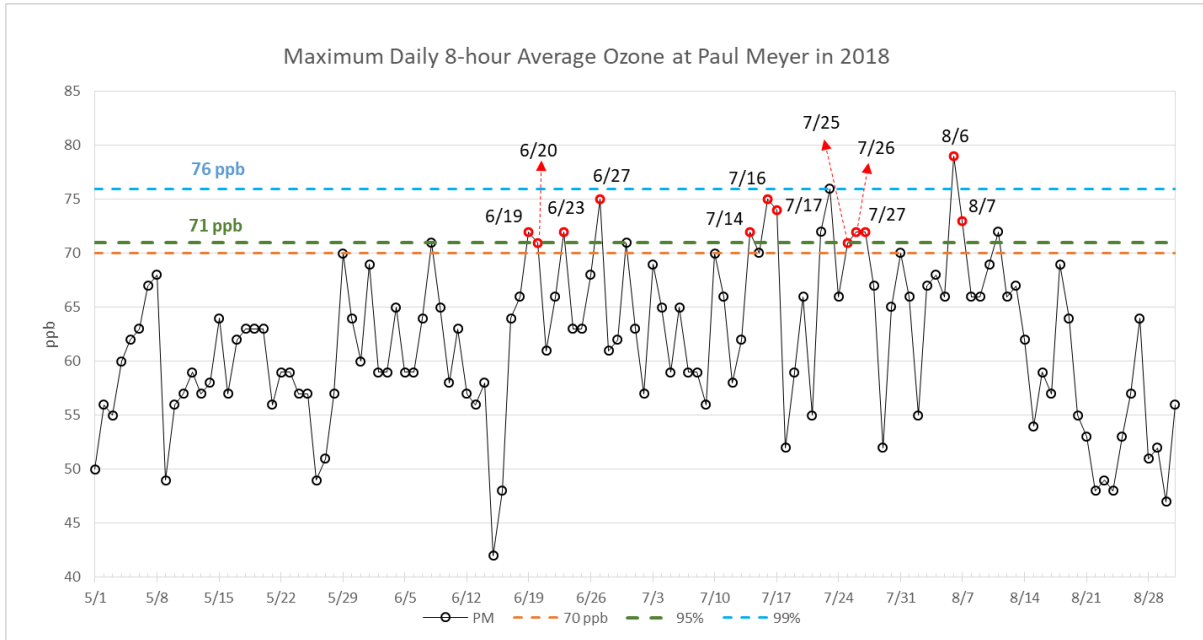


Figure 4-3. MDA8 Ozone at Paul Meyer, 2018 Ozone Season.

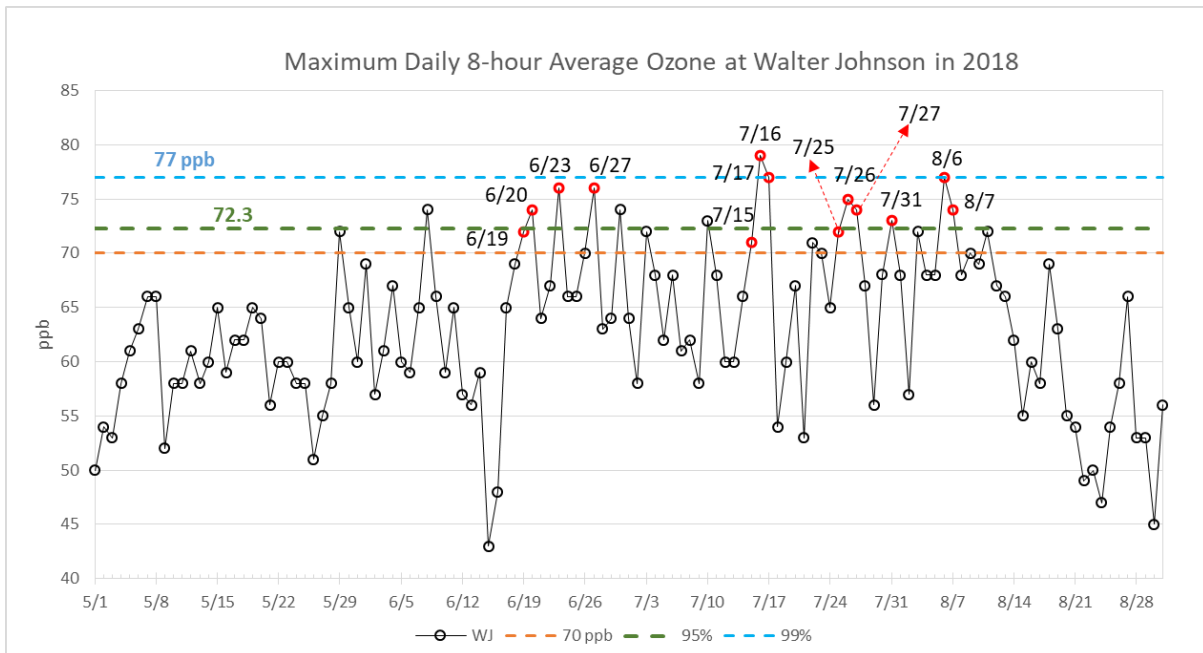


Figure 4-4. MDA8 Ozone at Walter Johnson, 2018 Ozone Season.

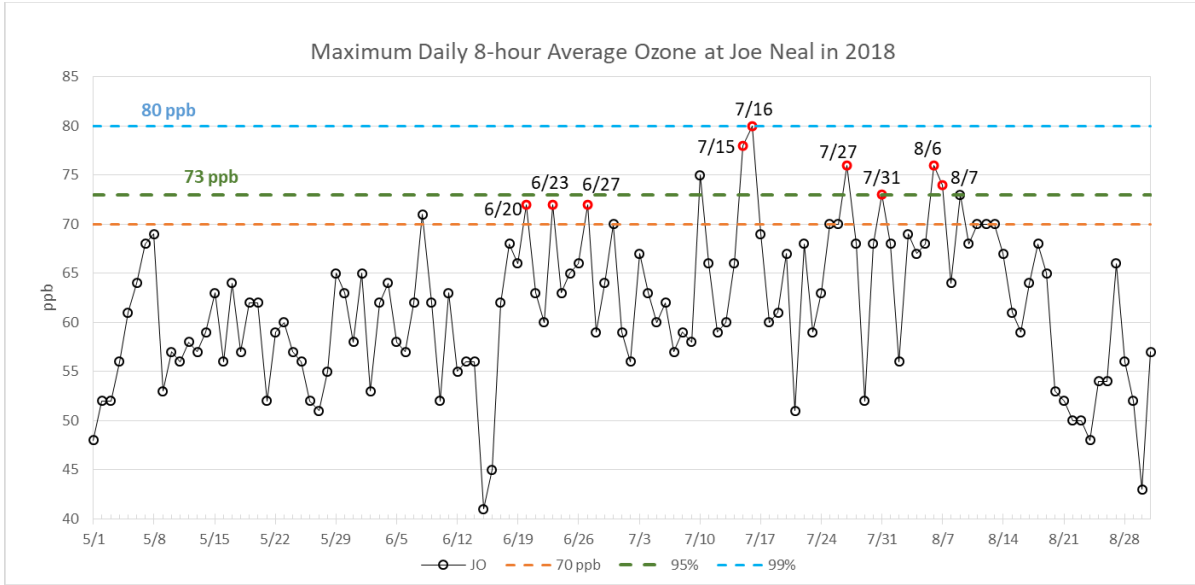


Figure 4-5. MDA8 Ozone at Joe Neal, 2018 Ozone Season.

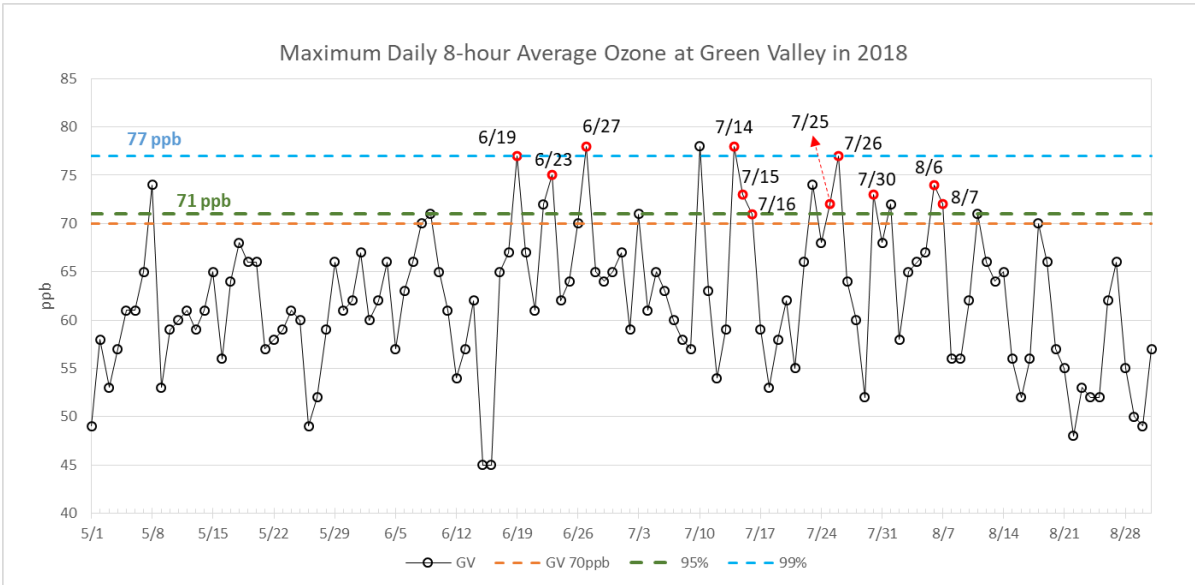


Figure 4-6. MDA8 Ozone at Green Valley, 2018 Ozone Season.

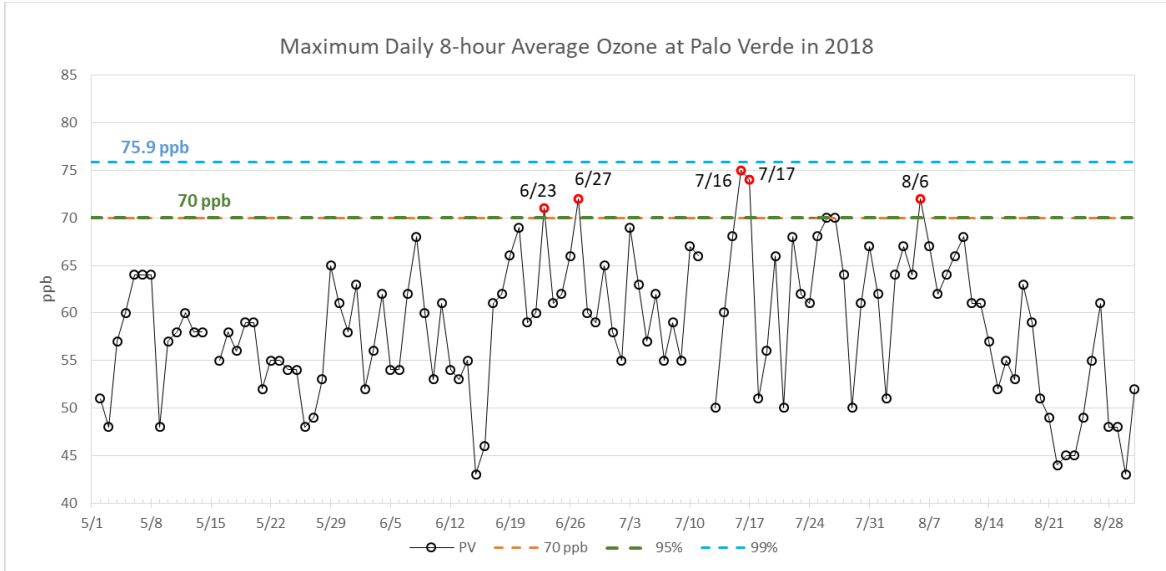


Figure 4-7. MDA8 Ozone at Palo Verde, 2018 Ozone Season.

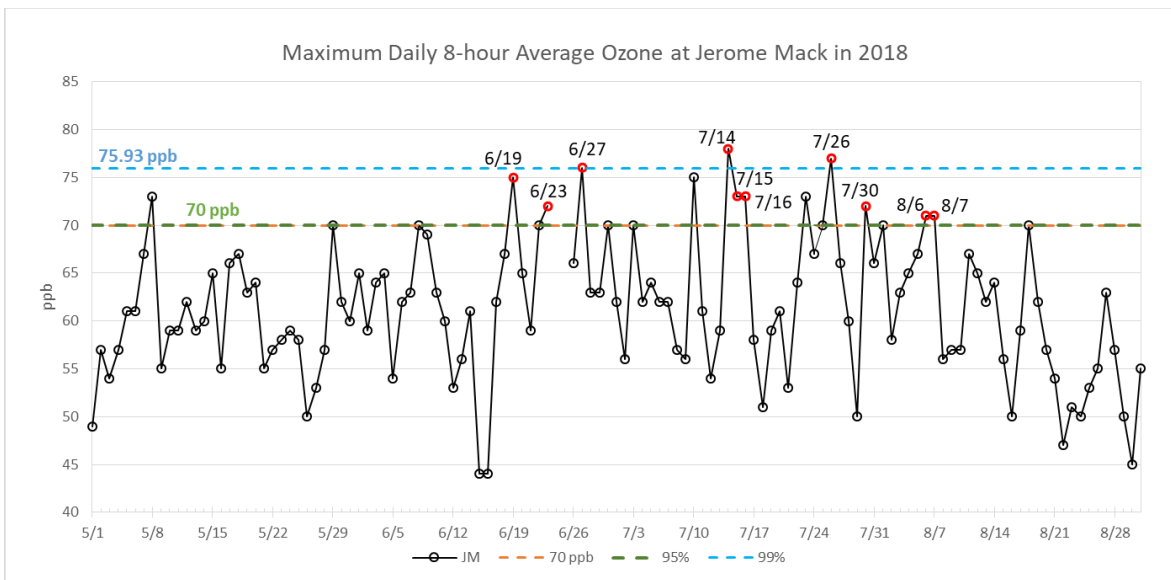


Figure 4-8. MDA8 Ozone at Jerome Mack, 2018 Ozone Season.

The ratio of PM_{2.5} organic carbon (OC) to elemental carbon (EC) has been used to differentiate combustion sources of biomass burning and mobile sources, since biomass burning usually has a higher OC/EC ratio (ranging between 7 and 15) (Lee et al. 2005; Pio et al. 2008) than gasoline (ranging between 3.0 and 4.0) or diesel vehicles (<1.0) (Lee and Russell 2007; Zheng et al. 2007). The acquired PM_{2.5} of OC and EC in the LVV from EPA’s Air Quality System (https://aq5.epa.gov/aq5web/airdata/download_files.html) is available only for Jerome Mack on a three-day sampling schedule.

Figure 4-9 shows the OC/EC ratio for May–August in 2018 and 2019 against the median OC/EC ratio for May–August (5.4, orange line) and September–April (3.4, green line) according to

2015–2017 and 2019 data. It clearly shows a larger wildfire influence in ozone season months than non-ozone season months, and more days impacted by wildfire during ozone season months in 2018 than 2019 (a clean year with the annual 4th highest MDA8 ozone for all monitors below the 2015 ozone NAAQS). Figure 4-10 shows a similar OC/EC ratio plot for an upwind monitor located at Rubidoux in the Riverside-San Bernardino, CA, area with the median value for May–August (6.8, orange line) and September–April (3.4, green line). The larger summer median OC/EC ratio at Rubidoux makes sense, considering the difference in distance to the California fires. Comparing Figures 4-9 and 4-10 shows the daily variation in the OC/EC ratio at JM generally follows the variation at Rubidoux, and that more days in 2018 than 2019 had an OC/EC ratio above the median value for both monitors. It strongly indicates Jerome Mack was frequently impacted by California wildfires in 2018.

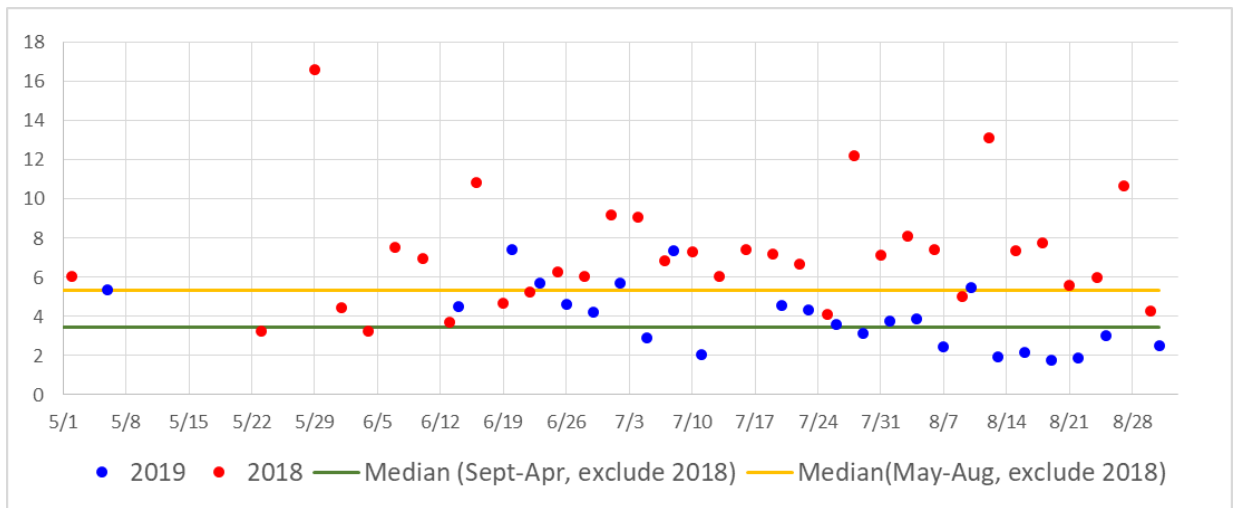


Figure 4-9. OC/EC Ratio at Jerome Mack, 2018–2019 Ozone Season.

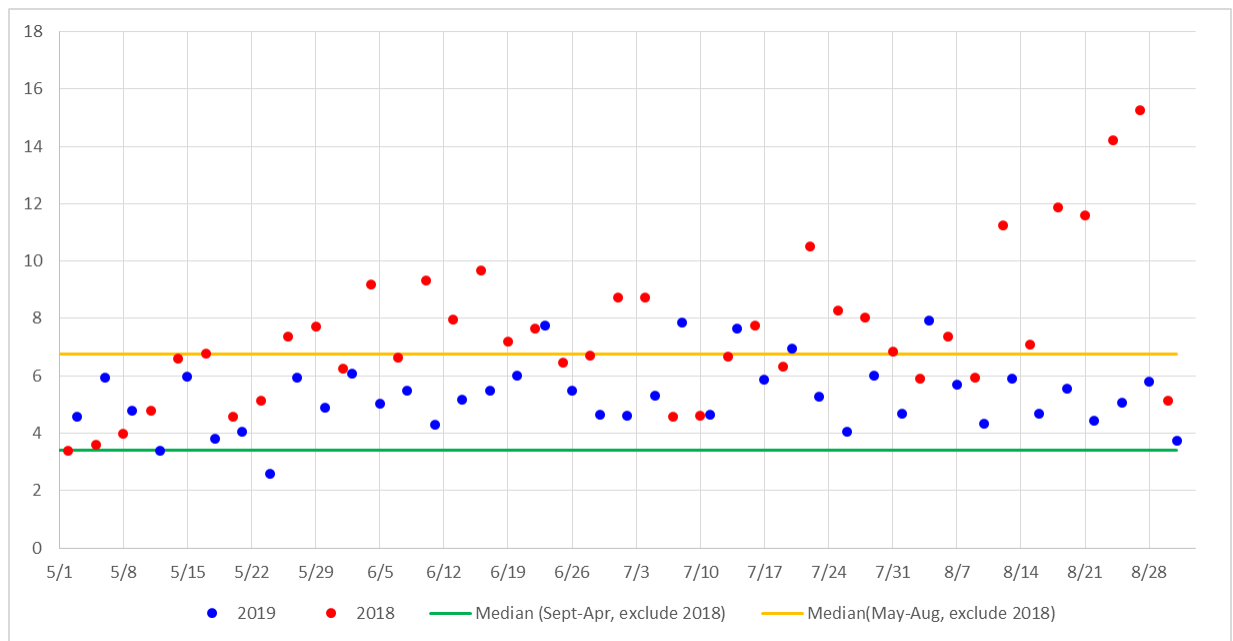


Figure 4-10. OC/EC ratio at Rubidoux, CA, 2018–2019 Ozone Season.

4.3 EVENT OF JUNE 27, 2018

4.3.1 Tier 1 Analysis: Historical Concentrations

Figure 4-11 shows the hourly seasonal percentiles for ozone from 2014–2018 compared to measured hourly ozone on June 27, 2018, at exceeding sites. O₃ levels at all exceeding sites but Joe Neal were above the 95th percentile with maximum difference 5~10 ppb, and the figure shows they were higher than non-event-related concentrations on June 27 for more than seven hours. Additionally, Figure 4-11 also shows multiple peaks in the nontypical ozone diurnal profiles; of special note is one peak that occurred in the early morning 2 A.M. ~ 3 A.M. before sunrise. Therefore, these data provide evidence of clear causal relationship between wildfire emissions and ozone exceedances.



Figure 4-11. 5-Year Hourly Seasonal 95th & 50th Percentiles for O₃ and Observed O₃ on June 27.

4.3.2 Tier 2 Analysis

4.3.2.1 Key Factor #2

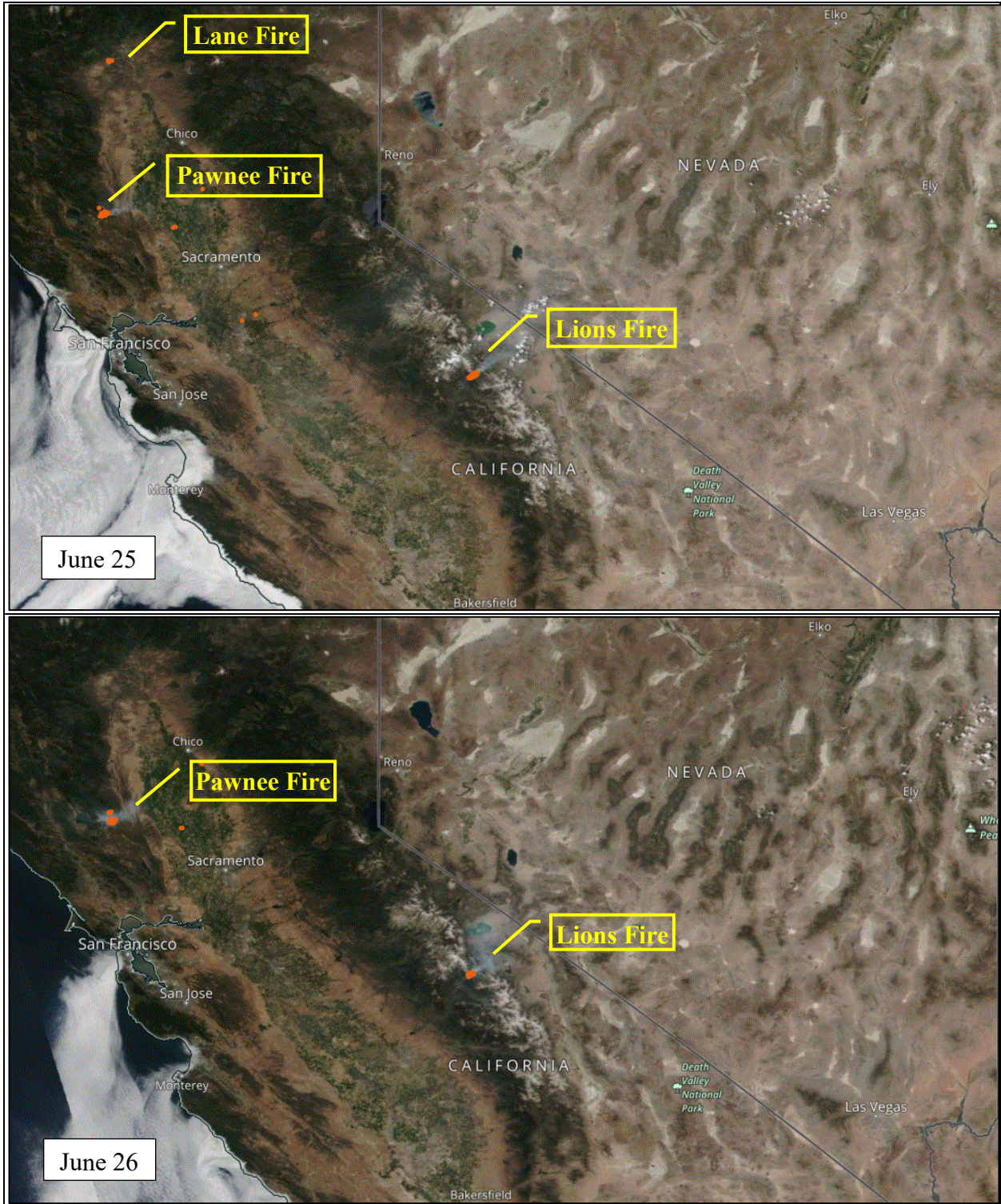
Figures 4-3 through 4-8 show that O₃ levels on June 27 were above the five-year 95th percentile values at all exceeding sites in HA 212 except Joe Neal (1 ppb below). The O₃ exceedances at Jerome Mack and Green Valley were equal to or above the five-year 99th percentile values, and those at Paul Meyer and Walter Johnson were only 1 ppb below the five-year 99th percentile values. All sites except Joe Neal recorded one of the four highest MDA8 ozone values (Table 1-1) for 2018, with Green Valley recording the highest. The Key Factor #2 analysis results thus do not completely meet the criteria to support a demonstration that the O₃ exceedance on June 27 was caused by an exceptional event, but are strong evidence of the presence of an extreme event.

4.3.2.2 Evidence of Fire Emissions Transport to Area Monitors

Visible Satellite Imagery

Visible satellite imagery from the MODIS Aqua and Terra satellites shows the dense smoke from the Lions, Pawnee, and Lane Fires in California on June 24–26 (Figure 4-12). Continuous smoke from wildfires was transported southward/southeastward during these days, as depicted in Figure 3-10. Therefore, wildfire emissions dominated the atmosphere in southern California.





Source: NASA Worldview.

Figure 4-12. Visible Satellite Imagery, June 24–26.

Satellite Retrieval—AOD Map

Examining the AOD maps for June 25–27 (Figures 4-13 to 4-15) shows that air movements during this period, as depicted in the conceptual model (Figure 3-10), transported smoke from fires in Oregon, California, and Mexico to southern Nevada and California desert areas. On June 25, the smoke from Oregon and northern California wildfires was transported on southeasterly winds to northern Nevada just as the smoke from wildfires in Mexico was being transported on northwesterly winds toward the LVV. Under the meteorological conditions favoring ozone formation (Figure 3-9) on June 26–27, this smoke continuously transported into and hovered over the LVV, contributing to the 2015 ozone NAAQS exceedance.

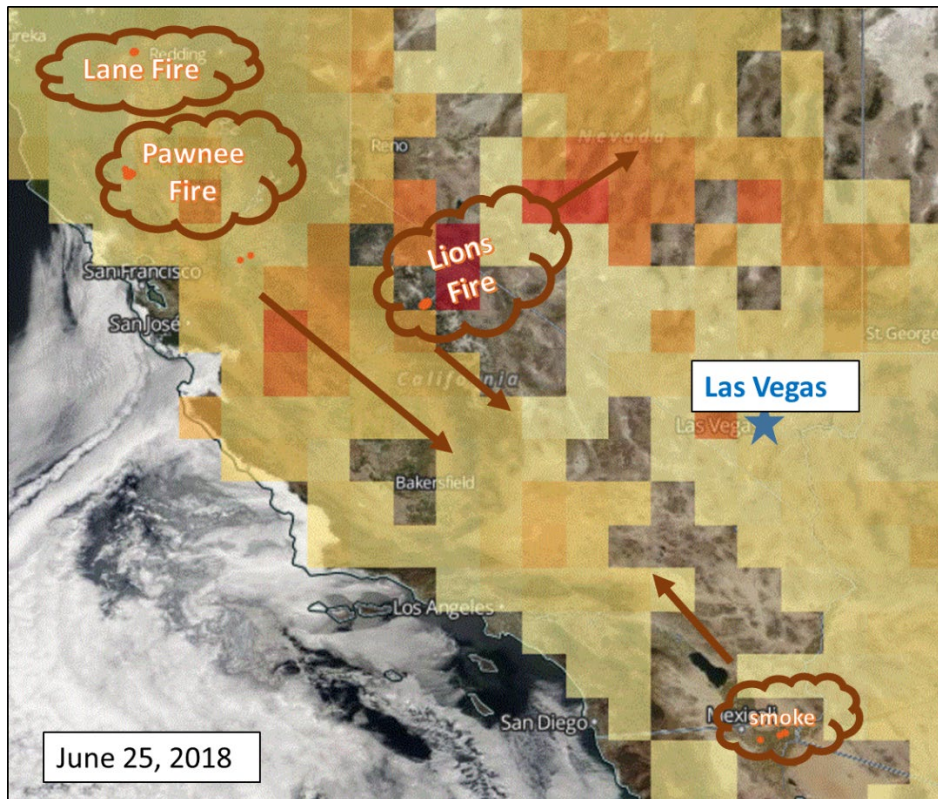


Figure 4-13. MODIS (Aqua/Terra) AOD Retrievals for June 25.

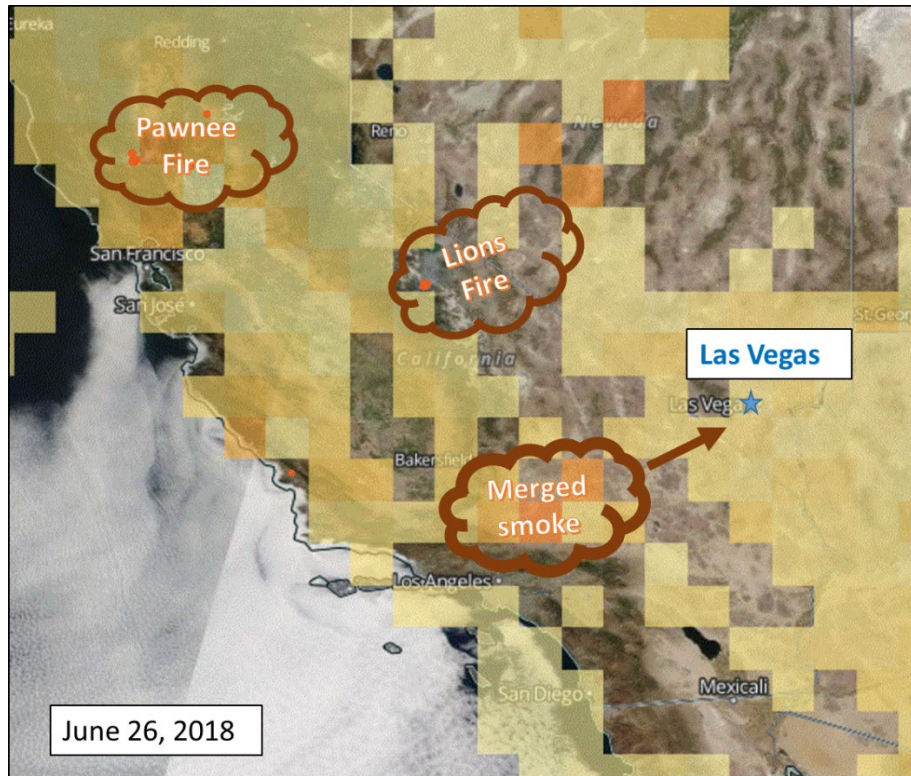


Figure 4-14. MODIS (Aqua/Terra) AOD Retrievals for June 26.

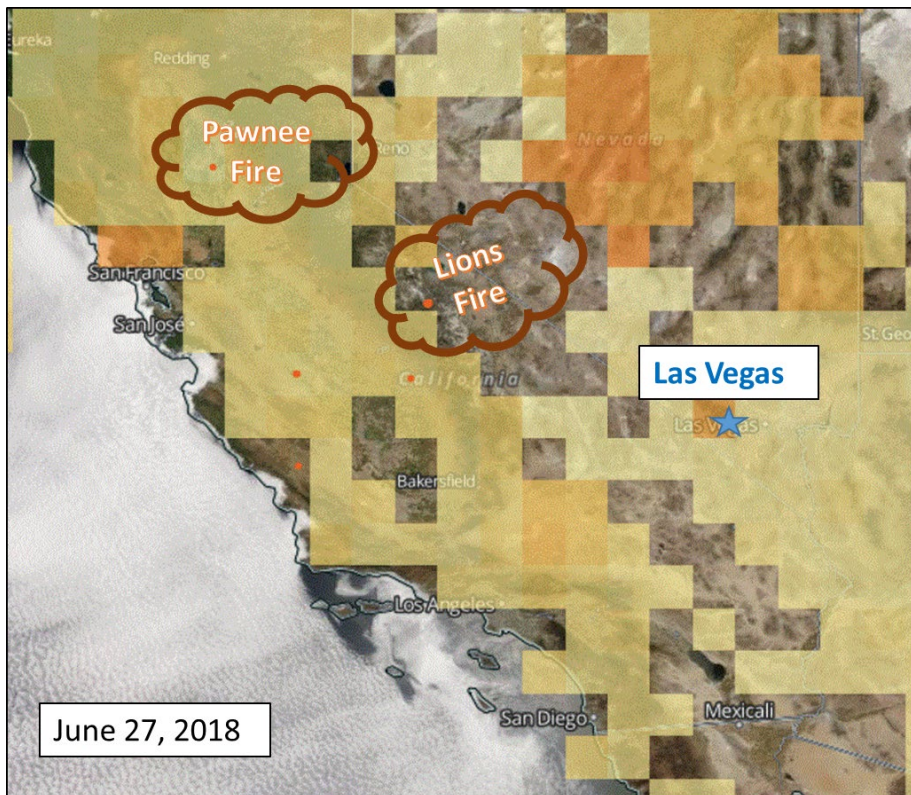
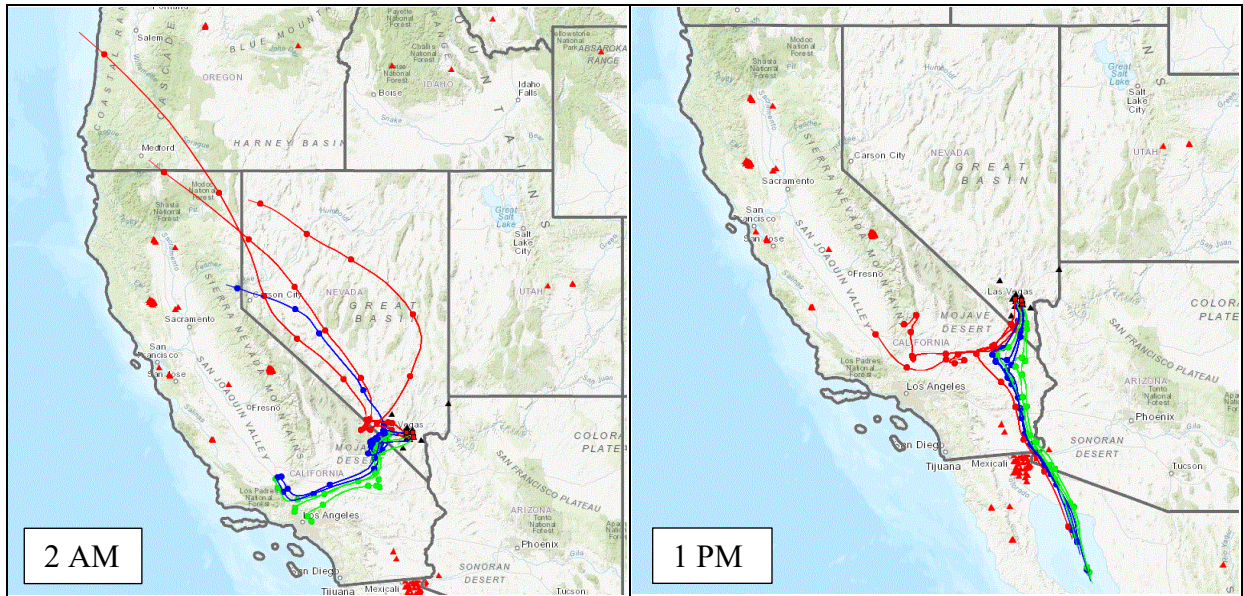


Figure 4-15. MODIS (Aqua/Terra) AOD Retrievals for June 27.

HYSPLIT Backward Trajectories

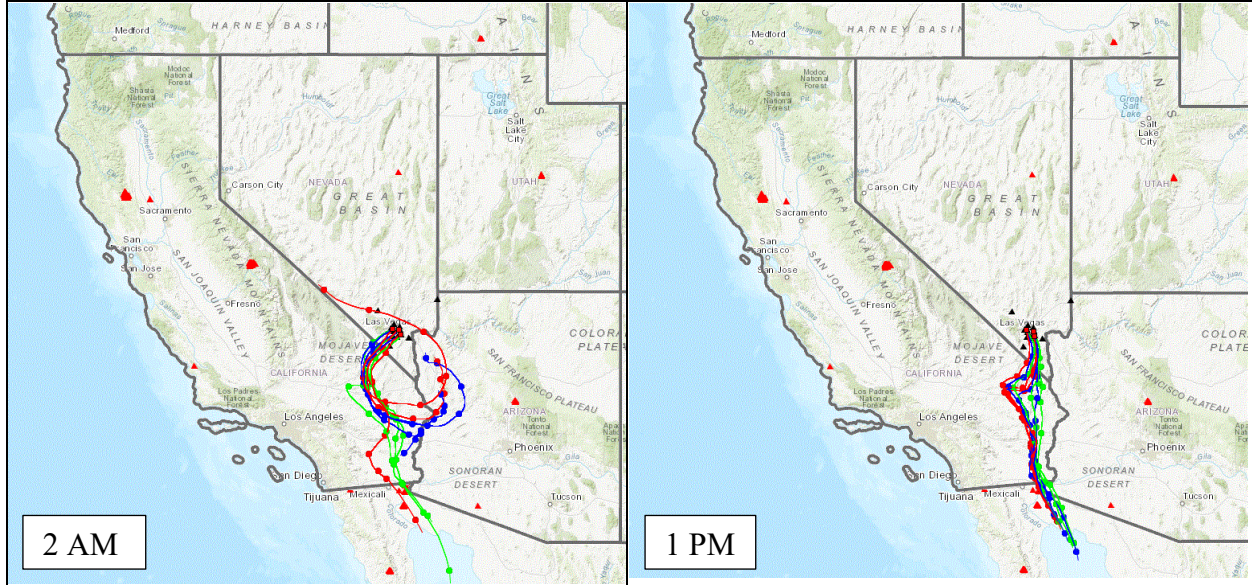
The NOAA HYSPLIT model was run to produce back trajectories of air parcel movement at 10, 500, and 1,000 m (EPA guidance recommends within 100~1,500 meters) for three exceeding monitors: Green Valley, Jerome Mack, and Walter Johnson. Green Valley and Walter Johnson, located on two sides of the urban core area, recorded the highest and fourth highest MDA8 ozone levels of 2018 on June 27. Jerome Mack, the NCore monitor, was selected not only because it recorded the third highest MDA8 ozone level of 2018, but also because it can measure many variables for analysis. Figures 4-16 to 4-18 show the 48-hour backward trajectories of airflows arriving at three monitors at 2 a.m. and 1 p.m. on June 25–27.

The figures show how the backward trajectories of airflows traveled predominantly from wildfire emission source regions—i.e., northern Nevada, northern/central California, and California/Mexico (Figure 3-4)—toward southern Nevada and the California deserts. The nocturnal residual layers on June 26–27 (Figure 3-8) were deep enough to cap the substantial continuous smoke transported to the LVV. Under the meteorological conditions favoring ozone formation (Figure 3-9) on June 26–27, additional ozone from the nocturnal layers elevated concentrations rapidly after sunrise at all monitors in HA 112, contributing to an exceedance of the 2015 ozone NAAQS.



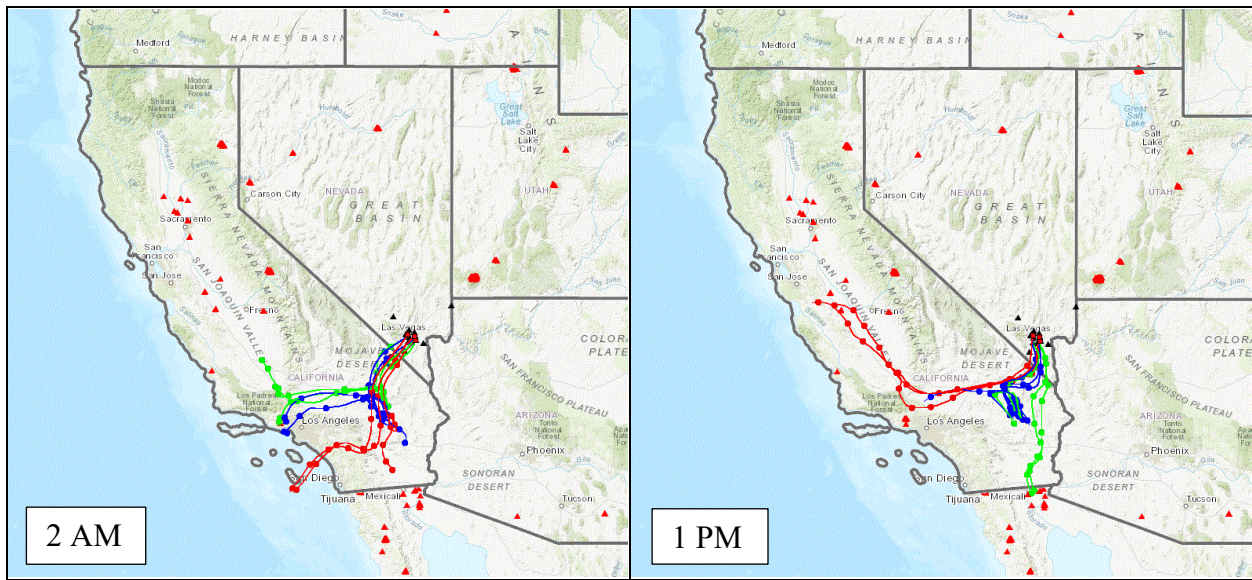
Note: Red = 1000 m, blue = 500 m, green = 10 m.

Figure 4-16. 48-hr Backward Trajectories at GV, JM, and WJ, 2 AM and 1 PM PST, June 25.



Note: Red = 1000 m, blue = 500 m, green = 10 m.

Figure 4-17. 48-hr Backward Trajectories at GV, JM, and WJ, 2 AM and 1 PM PST, June 26.



Note: Red = 1000 m, blue = 500 m, green = 10 m.

Figure 4-18. 48-hr Backward Trajectories at GV, JM, and WJ, 2 AM and 1 PM PST, June 27.

4.3.2.3 Evidence that Fire Emissions Affected Area Monitors

Concurrent Rise in Ozone Concentrations

We examined MDA8 O₃ at monitors inside (Figure 2-2) and outside (Figure 4-19) the LVV on June 25–28, 2018 (Figures 4-20 & 4-21).



Figure 4-19. Monitors Outside the Las Vegas Valley.

Visible satellite imagery, AOD maps, backward trajectories, and the meteorological conditions detailed in Section 3.3 depict the transport of smoke, ozone, and ozone precursor emissions from wildfires in Oregon, central/ northern California, northern Nevada, and Mexico to the LVV.

Figure 4-20 shows MDA8 O₃ at upwind monitors (Death Valley, Mojave, and Jean) increasing gradually from June 25 to June 27. MDA8 O₃ at the Death Valley and Mojave monitors, especially, was higher than the 95th percentile value starting on June 25, but the widespread smoke also impacted O₃ readings at rural monitors (Great Basin and Mesquite) on June 27.

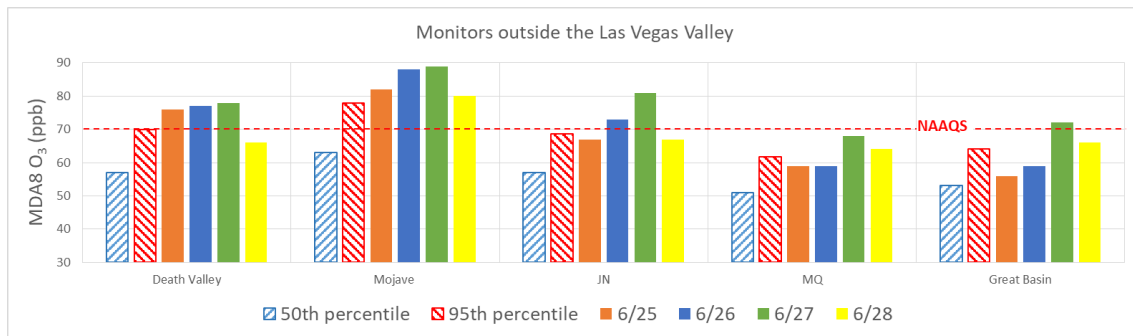


Figure 4-20. MDA8 O₃ at Monitors Outside the LVV, June 25–28.

Figure 4-21 shows that monitors in the LVV had a similar daily increment of MDA8 O₃ as the upwind monitors on June 25–27 due to the influence of wildfire smoke.

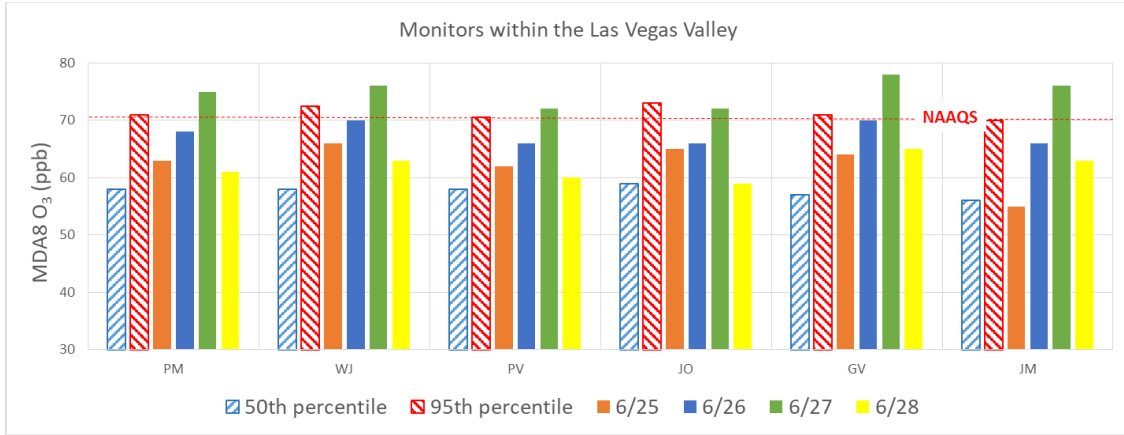


Figure 4-21. MDA8 O₃ at Monitors Inside the LVV, June 25–28.

Additionally, ozone measurements for June 25–28 from the Death Valley and Great Basin monitors (Figure 4-22 and 4-23) reflect continuous smoke impacts from wildfire emission-rich areas during this period.

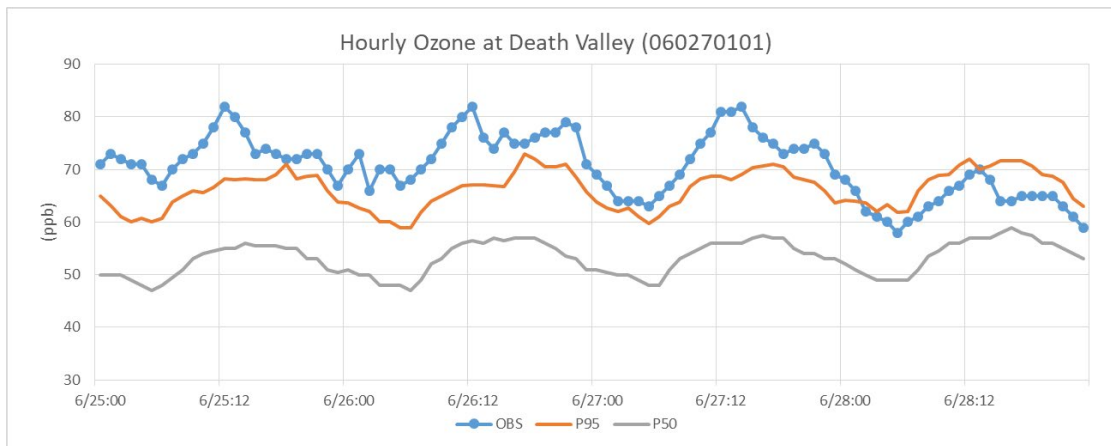


Figure 4-22. Time Series of 1-Hour Ozone Readings for Death Valley, June 25–28.

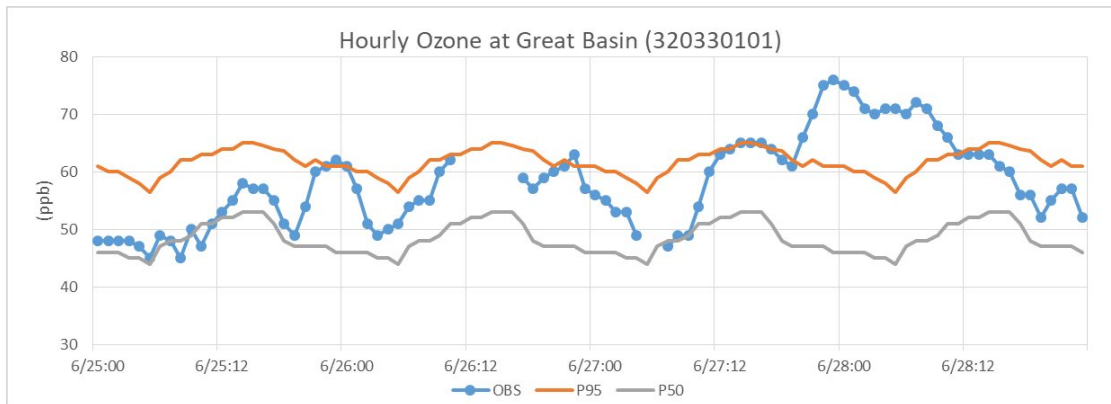


Figure 4-23. Time Series of 1-Hour Ozone Readings for Great Basin, June 25–28.

Analysis of PM_{2.5} Speciation Data

Section 4.2 describes how the ratio of OC to EC can be used to differentiate combustion sources of biomass burning from mobile sources. Figure 4-24 shows the actual and mean OC/EC ratio at Jerome Mack and Rubidoux, CA, and daily 24-hour PM_{2.5} levels at Jerome Mack. The OC/EC ratio at Jerome Mack on June 25 and 28 was above its normal summer OC/EC ratio; the OC/EC ratios for Rubidoux did not exceed, but were very close to the average summer value. Therefore, this analysis provides evidence the presence of wildfire smoke did influenced ozone levels in the LVV.

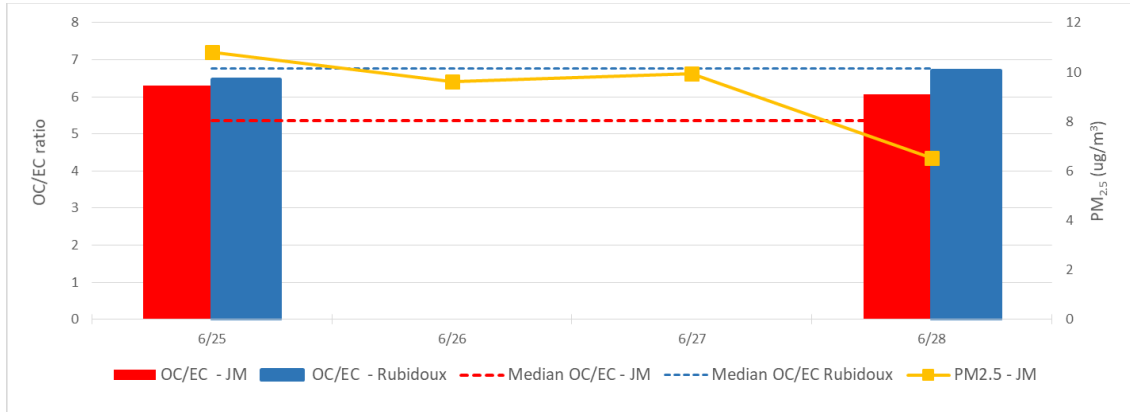


Figure 4-24. Actual and Mean OC/EC ratio at Jerome Mack and Rubidoux, CA, and Daily 24-hour PM_{2.5} at Jerome Mack, June 25–28, 2018.

Analysis of Levoglucosan

The best available PM_{2.5} sample for levoglucosan analysis was collected on June 28. The analysis result was 0.0023 µg/m³ for Sunrise Acres (no sample is available for Jerome Mack), indicating that smoke very likely was already present in the LVV before June 28.

Supporting Ground Measurements

Ground measurements of wildfire plume components (e.g., PM_{2.5}, NO₂) can be used to demonstrate that smoke impacted ground-level air quality if elevated concentrations or unusual diurnal patterns are observed. Jerome Mack is the only monitor that records all four pollutants, and its MDA8 O₃ on June 27, 2018, was 76 ppb.

Because CO measurements are not available for June 25–28, Figures 4-25 to 4-27 show hourly levels of only O₃, NO₂, and PM_{2.5}. Still, these figures clearly show the impact of wildfire smoke, which caused a large increase in NO₂ and PM_{2.5} concentrations in the early morning hours of June 25–27 and a substantial rise in O₃ concentrations in the hours before noon because of additional residual ozone. Similarly, the impact of wildfire smoke on O₃, NO₂, and PM_{2.5} concentrations can be seen throughout this period as wildfire smoke transported into the LVV intermittently.

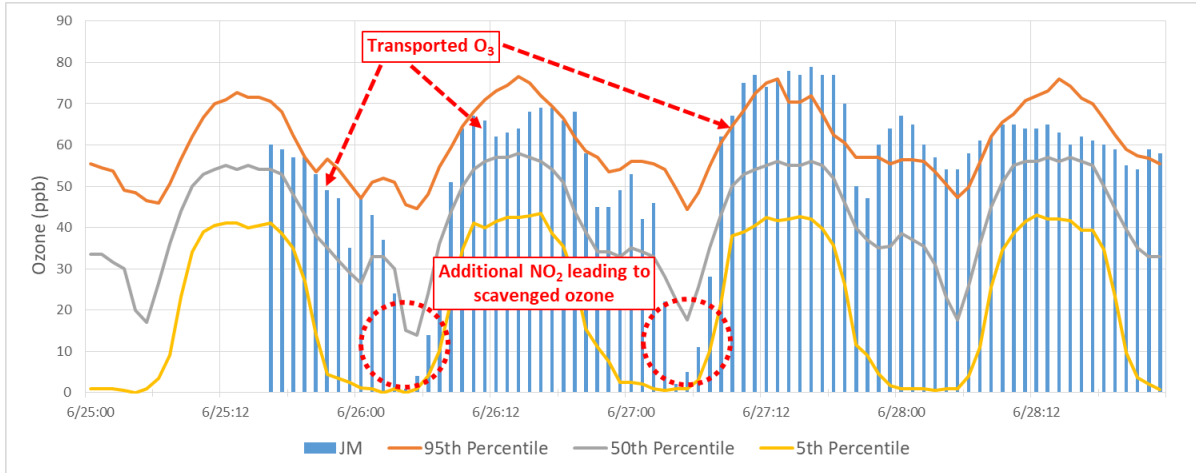


Figure 4-25. Hourly O₃ Concentrations at Jerome Mack, June 25–28.

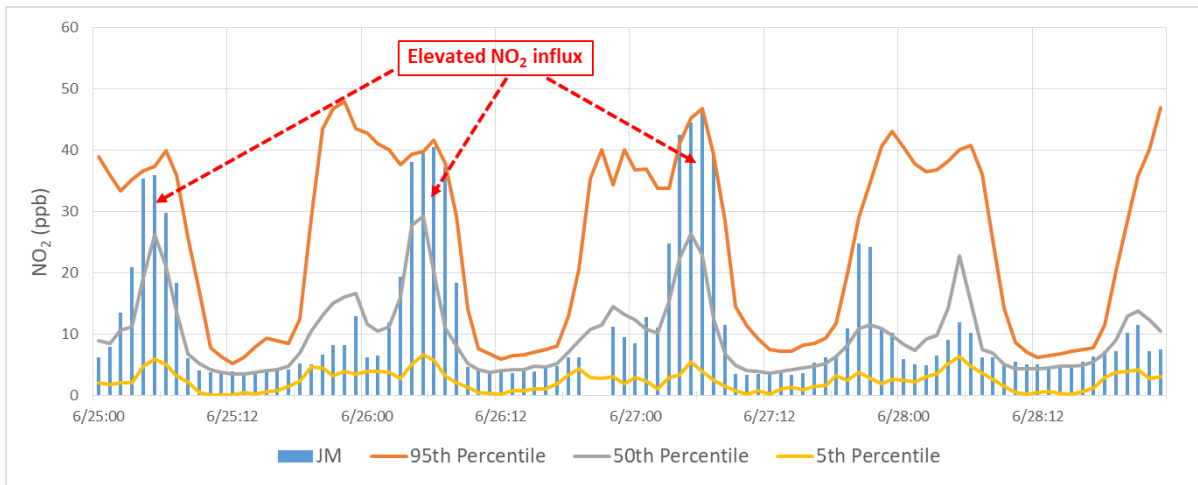


Figure 4-26. Hourly NO₂ Concentrations at Jerome Mack, June 25–28.

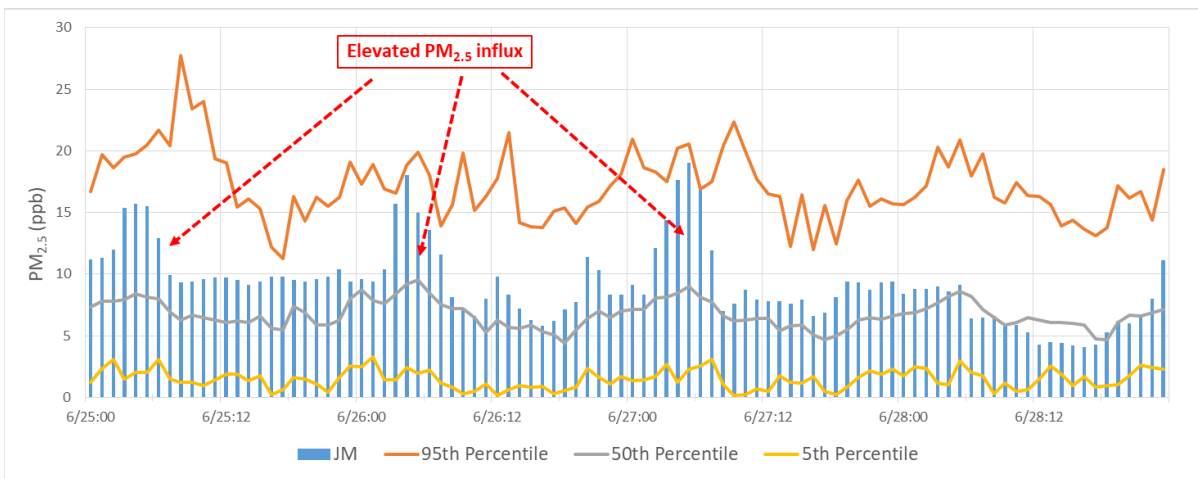


Figure 4-27. Hourly PM_{2.5} Concentrations at Jerome Mack, June 25–28.

4.3.3 Tier 3 Analysis: Additional Weight of Evidence to Support Clear Causal Relationship

4.3.3.1 GAM Statistical Modeling

Figure 4-28 shows a time series of predicted and observed MDA8 O₃ for June 24–28, 2018. Lacking predictors for June 25, no GAM prediction was calculated. The results indicate the monitors would normally not have exceeded the 2015 NAAQS under the meteorological conditions on June 27, suggesting that a variable outside the norm (e.g., increased emissions from wildfires) influenced ozone concentrations. Table 4-1 lists GAM results for June 27, 2018, at the exceeding monitors petitioned for data exclusion from normal planning and regulatory requirements. GAM residuals show a modeled wildfire impact of between 6.7 and 9.1 ppb for exceeding monitors, with GAM MDA8 O₃ prediction values all below the 70 ppb standard.

EPA guidance recommends using an additional step to estimate the ozone contribution from a wildfire: the difference between the observed ozone and the sum of predicted ozone + positive 95th percentile value. Simply speaking, the residuals on the wildfire event day would have to be greater than the positive 95th percentile value to see any wildfire contributions to ozone concentrations. Table 4-1 shows that none of the residuals exceed the 95th percentile value for June 27. However, two issues with this methodology must be considered.

First, a large number of wildfires affecting Clark County from 2014–2020 (especially in 2018 and 2020) included in GAM modeling cause a very conservative 95th percentile value (positive). Second, given the limitations of regression analysis for ozone production—which involves complex physical and chemical processes regarding emissions and meteorological conditions—models are able to explain about 50% of the correlation between predicted and observed concentrations (see Table 3-16 in *Exceptional Event Demonstration for Ozone Exceedances in Clark County, Nevada—June 22, 2020*), which is typical of the results seen in other regression analysis studies.

The percentile ranks of positive residuals for June 27 for the exceeding monitors range from 78th to 92nd (Table 4-1). The model indicates a 8% ~ 22% chance that the residuals at exceeding monitors would be produced under the meteorological conditions on June 27, suggesting likely additional emissions (e.g., wildfires) are not counted. As Section 3.3 describes, weather conditions on June 27 were stable and favored ozone formation. Additional wildfire emissions helped to drive already elevated ozone concentrations to exceed the 2015 NAAQS on June 27.

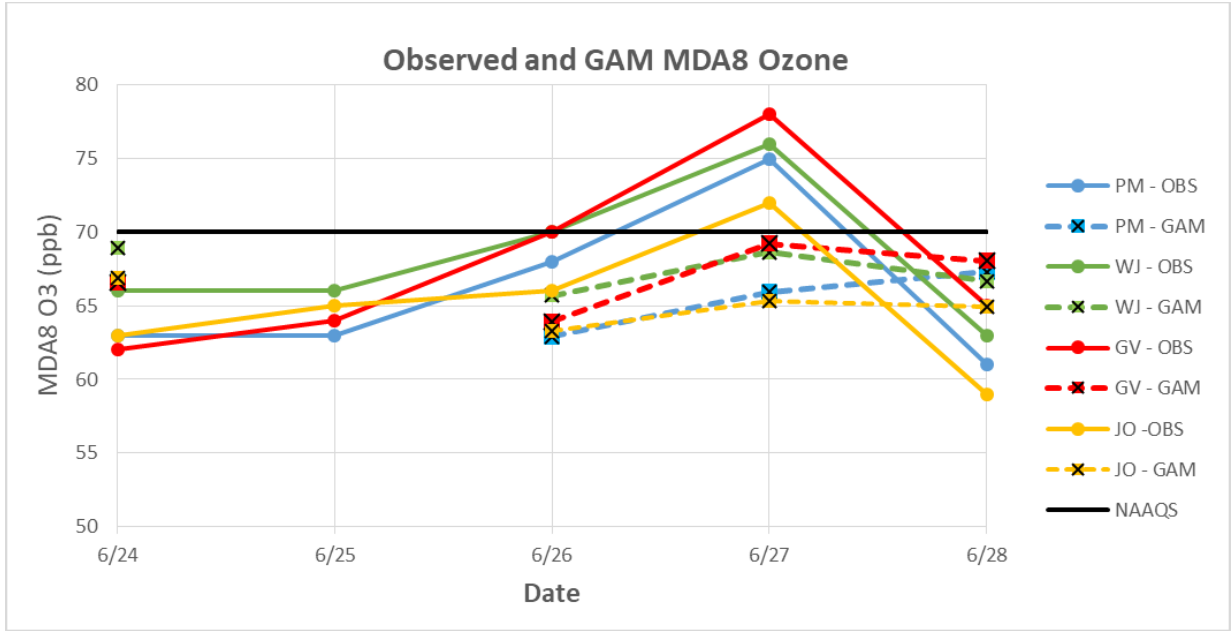


Figure 4-28. Observed and Predicted MDA8 O₃ at Exceeding Monitors, June 24–28.

Table 4-1. June 27 GAM Results for Exceeding Sites

| Date | Site | MDA8 O ₃ (ppb) | MDA8 GAM Prediction (ppb) | GAM Residual (ppb) | Positive 95 th Quantile (ppb) | Predicted Fire Influence | Percentile Rank of Positive Residual |
|-----------|----------------|---------------------------|---------------------------|--------------------|--|--------------------------|--------------------------------------|
| 6/27/2018 | Paul Meyer | 75 | 65.9 | 9.1 | 10.5 | -1.5 | 91st |
| | Walter Johnson | 76 | 68.6 | 7.4 | 10.8 | -3.5 | 85th |
| | Joe Neal | 72 | 65.3 | 6.7 | 10.6 | -3.9 | 78th |
| | Green Valley | 78 | 69.2 | 8.8 | 10.1 | -1.3 | 92nd |

5.0 NATURAL EVENT

40 CFR 50.14(c)(3)(iv)(E) requires that agencies demonstrate an “event was a human activity that is unlikely to recur at a particular location or was a natural event.” 40 CFR 50.1(k) defines a natural event as “an event and its resulting emissions, which may recur at the same location, in which human activity plays little or no direct causal role.” 40 CFR 50.1(n) defines a wildfire as “any fire started by an unplanned ignition caused by lightning; volcanoes; other acts of nature; unauthorized activity; or accidental, human-caused actions, or a prescribed fire that has developed into a wildfire. A wildfire that predominantly occurs on wildland is a natural event.” And lastly, 40 CFR 50.1(o) defines wildland as an “area in which human activity and development are essentially non-existent, except for roads, railroads, power lines, and similar transportation facilities. Structures, if any, are widely scattered.”

Based on the documentation provided in Section 3, the event that occurred on June 27 falls within the definition of a natural event (40 CFR 50.1(k)). As demonstrated, these wildfires were caused by lightning or human activity and occurred predominantly on wildland, as detailed in Table 5-1, meeting the regulatory definitions outlined in 40 CFR 50.1(n) and (o). DES therefore concludes that these wildfire events can be treated as natural events under the EER.

Table 5-1. Basic Information for Wildfire Event on June 27, 2018

| Event Date(s) | Fire | Cause | Location–County (State) |
|----------------------|---------------------|--------------|--------------------------------|
| June 27 | Lions Fire | Unknown | Madera (CA) |
| | Pawnee Fire | Unknown | Lake (CA) |
| | Lane Fire | Unknown | Tehama (CA) |
| | Mexico border fires | Unknown | Mexico-CA border |

6.0 NOT REASONABLY CONTROLLABLE OR PREVENTABLE

Based on the documentation provided in Section 3, lightning and human activity (as defined in 40 CFR 50.1(n)) caused the wildfires on wildland (Table 5-1) that influenced ozone concentrations in the LVV on June 27, 2018. DES is not aware of any evidence clearly demonstrating that prevention and control efforts beyond those actually made would have been reasonable; therefore, emissions from these wildfires were not reasonably controllable or preventable.

7.0 CONCLUSIONS

The analyses reported in this document support the conclusion that smoke from wildfires impacted ozone concentrations in Clark County, Nevada, on the event day of June 27, 2018. Specifically, this document has used the following evidence to demonstrate the exceptional event:

- Statistical analyses of the monitoring data compared to historical concentrations support the conclusion of unusual and above-normal historical concentrations at monitoring sites.
- Visible satellite imagery and AOD maps support the conclusion that smoke was transported to LVV monitoring sites.
- Backward trajectories support the conclusion of transport of smoke from wildfires to LVV monitoring sites.
- Enhanced ground measurements of wildfire plume components (PM_{2.5}, NO₂, and CO) and OC/EC ratios support the conclusion that ozone concentrations at LVV monitoring sites were impacted by smoke from wildfires.
- Aerosols in vertical profile and sounding data support the conclusion that smoke was mixed down to the surface in Clark County.
- Comparisons with non-event concentrations and GAM statistical modeling support the conclusion that ozone concentrations in Clark County were well above typical summer concentrations.

Based on the evidence presented in this package, the wildfires on June 27, 2018, in Clark County were natural events and unlikely to recur. The analyses described satisfy the clear causal relationship criterion for recognition as an exceptional event. Based on this evidence, DES requests that EPA exclude the data recorded at the Green Valley, Joe Neal, Walter Johnson, and Paul Meyer monitors on June 27, 2018, from use for regulatory determinations.

8.0 REFERENCES

- Bhattacharai H., Saikawa E., Wan X., Zhu H., Ram K., Gao S., Kang S., Zhang Q., Zhang Y., Wu G., Wang X., Kawamura K., Fu P., and Cong Z. (2019) Levoglucosan as a tracer of biomass burning: recent progress and perspectives. *Atmospheric Research*, 220, 20-33, doi: 10.1016/j.atmosres.2019.01.004. Available at <http://www.sciencedirect.com/science/article/pii/S0169809518311098>.
- Butler, T.J., Vermeylen F.M., Rury M., Likens G.E., Lee B., Bowker G.E., and McCluney L. 2011. "Response of ozone and nitrate to stationary source NO_x emission reductions in the eastern USA." *Atmospheric Environment*, 45(5), 1084-1094, doi:Doi 10.1016/J.Atmosenv.2010.11.040.
- DES. 2008. *Southwest Desert/Las Vegas Ozone Transport Study (SLOTS)*. Las Vegas, NV: Clark County Department of Environment and Sustainability.
- DES. 2013. *Las Vegas Ozone Study (LVOS)*. Las Vegas, NV: Clark County Department of Environment and Sustainability.
- DES. 2017. *Fires, Asia, and Stratospheric Transport Las Vegas Ozone Study (FAST-LVOS)*. Las Vegas, NV: Clark County Department of Environment and Sustainability.
- EPA. 2012. "Our Nation's Air: Status and Trends through 2010." U.S. Environmental Protection Agency, EPA-454/R-12-001. Research Triangle Park, NC: Office of Air Quality Planning and Standards.
- EPA. 2016. "Guidance on the Preparation of Exceptional Events Demonstrations for Wildfire Events that May Influence Ozone Concentrations." U.S. Environmental Protection Agency memo. Research Triangle Park, North Carolina.
- He, H. et al. 2013. "Trends in emissions and concentrations of air pollutants in the lower troposphere in the Baltimore/Washington airshed from 1997 to 2011." *Atmos. Chem. Phys.*, 13(15), 7859-7874, doi:10.5194/acp-13-7859-2013.
- Hennigan C.J., Sullivan A.P., Collett J.L., Jr., and Robinson A.L. (2010) Levoglucosan stability in biomass burning particles exposed to hydroxyl radicals. *Geophysical Research Letters*, 37(L09806), doi: 10.1029/2010GL043088. Available at https://www.firescience.gov/projects/09-1-03-1/project/09-1-03-1_hennigan_etal_grl_2010.pdf.
- Hoffmann D., Tilgner A., Iinuma Y., and Herrmann H. (2009) Atmospheric stability of levoglucosan: a detailed laboratory and modeling study. *Environ. Sci. Technol.*, 44, 694–699.
- Jaffe, D.A., Bertschi I., Jaegle L., Novelli P., Reid J.S., Tanimoto H., Vingarzan R., and Westphal D.L. 2004. "Long-range transport of Siberian biomass burning emissions and impact on surface ozone in western North America." *Geophys. Res. Lett.*, 31(L16106).

Lai C., Liu Y., Ma J., Ma Q., and He H. (2014) Degradation kinetics of levoglucosan initiated by hydroxyl radical under different environmental conditions. *Atmos. Environ.*, 91, 32-39, doi: 10.1016/j.atmosenv.2014.03.054, 2014/07/01/. Available at <http://www.sciencedirect.com/science/article/pii/S1352231014002398>.

Lee, S., Baumann, K., Schauer, J.J., Sheesley, R.J., Naeher, L.P., Meinardi, S., Blake, D.R., Edgerton, E.S., Russell, A.G., Clements, M., 2005. "Gaseous and particulate emissions from prescribed burning in Georgia." *Environmental Science and Technology* 39, 9049-9056.

Lee, S., Russell, A.G., 2007. "Estimating uncertainties and uncertainty contributors of CMB PM2.5 source apportionment results." *Atmospheric Environment* 41, 9616-9624.

Lefohn, A., Shadwick D., and Oltmans S. 2010. "Characterizing changes in surface ozone levels in metropolitan and rural areas in the United States for 1980-2008 and 1994-2008." *Atmos. Environ.*, 44, 5199-5210

Nikolov, N. 2008. "Impact of Wildland Fires and Prescribed Burns on Ground Level Ozone Concentration." Paper presented at the Western Regional Air Partnership Workshop on Regional Emissions & Air Quality Modeling Studies, July 30, 2008, Denver, CO.

Pace, T.G., and Pouliot, G. 2007. "EPA's Perspective on Fire Emission Inventories—Past, Present, and Future." Paper presented at the 16th Annual International Emission Inventory Conference (*Emission Inventories: Integration, Analysis, and Communications*), May 14-17, 2007, Raleigh, NC.

Pfister, G.G., Wiedinmyer C., and Emmons L.K. 2008. "Impact of the 2007 California wildfires on surface ozone: integrating local observations with global model simulations." *Geophysical Research Letters*, 35, L19814. doi:10.1029/2008GL034747.

Pio, C.A., Legrand, M., Alves, C.A., Oliveira, T., Afonso, J., Caseiro, A., Puxbaum, H., Sanchez-Ochoa, A., Gelensser, A., 2008. "Chemical composition of atmospheric aerosols during the 2003 summer intense forest fire period." *Atmospheric Environment* 42, 7530-7543.

Rowson, D. and Colucci S. 1992. "Synoptic Climatology of Thermal Low-Pressure Systems over South-Western North America." *International Journal of Climatology*, vol. 12: 529-545.

Sonoma Technology. 2020. "Exceptional Event Demonstration for Ozone Exceedances in Clark County, Nevada—August 18-21, 2020." Section 3.3.2. Petaluma, CA: Sonoma Technology.

Stewart, J., Whiteman C., Steenburgh W., and Bian X. 2002. "A climatological study of thermally driven wind systems of the U.S. intermountain west." *Bulletin of the American Meteorological Society* 83, 699-708

Wood, S.N. 2017. *Generalized Additive Models: An Introduction with R*. 2nd edition. Boca Raton, FL: CRC Press.

Zheng, M., Cass, G.R., Ke, L., Wang, F., Schauer, J.J., Edgerton, E.S., Russell, A.G., 2007. "Source apportionment of daily fine particulate matter at Jefferson street, Atlanta, GA, during summer and winter." *Journal of the Air and Waste Management Association* 57, 228-242.